NASA

Technical Memorandum **82065**

# Resonant Electrodynamic Heating of Stellar Coronal Loops: An LRC Circuit Analogue

**James A. Ionson**



**DECEMBER 1980**

National Aeronautics and
Space Administration

**Goddard Space Flight Center**
Greenbelt, Maryland 20771

# RESONANT ELECTRODYNAMIC HEATING OF STELLAR CORONAL LOOPS: AN LRC CIRCUIT ANALOGUE

James A. Ionson
Laboratory for Astronomy and Solar Physics
NASA-Goddard Space Flight Center
Greenbelt, Maryland 20771, USA

December 1980

# RESONANT ELECTRODYNAMIC HEATING OF STELLAR CORONAL LOOPS: AN LRC CIRCUIT ANALOGUE

James A. Ionson
Laboratory for Astronomy and Solar Physics
NASA-Goddard Space Flight Center
Greenbelt, Maryland 20771, USA

## Abstract

This article addresses the important problem of electrodynamic coupling of $\beta<1$ stellar coronal loops to underlying $\beta\gtrsim 1$ velocity fields. A rigorous analysis has revealed that the physics can be represented by a simple yet *equivalent* LRC circuit analogue. This analogue points to the existence of global structure oscillations which resonantly excite internal field line oscillations at a spatial resonance within the coronal loop. Although the width of this spatial resonance, as well as the induced currents and coronal velocity field, explicitly depend upon viscosity and resistivity, the *resonant* form of the generalized electrodynamic heating function is virtually *independent* of irreversibilities. This is a classic feature of high quality resonators that are externally driven by a broad-band source of spectral power.

The major results of this article are:

(1) The heating function, $E_H$, field-aligned electron current, and cross-field ion polarization current are explicit functions of the $\beta\gtrsim 1$ velocity field's spectral power function, e.g., $E_H=6.28\times10^{9}(T_{eff}/\ell^{2}_{cor})(R_{loop}/R_{global})\langle\tfrac{1}{2}\rho v^{2}_{\theta}\rangle^{photo}\nu_o$ (ergs/cm$^3$-sec). The essential feature of a resonant heating mechanism is that magnetic loops with different lengths, and hence different global resonance frequencies, are heated at a rate that critically depends upon the amount of spectral

power found at the resonance frequency, $\nu_o$.

(2) This heating function results in the following implicit equations for the maximum temperature, T, and base pressure, P:

$$T = 3.36 \times 10^4 \left[ T_{eff} \exp\left(0.36 \ell_{cor}/\ell_p\right) < 1/2 \rho v_\theta^2 >_{\nu_o}^{photo} \right]^{2/7} {}^{o}K$$

$$P = \frac{1.38 \times 10^4}{\ell_{cor}} \exp\left(1.51\, \ell_{cor}/\ell_p\right) \left[ T_{eff} < 1/2\, \rho v_\theta^2 >_{\nu_o}^{photo} \right]^{6/7} \left(\text{dynes/cm}^2\right)$$

which are in remarkable agreement with observations of solar coronal loops.

(3) Solar applications require nonlinear modifications that do not alter (1) and (2) above but which dramatically increase the cross-field size of the coronal dissipation site from kilometers to *thousands* of kilometers. Preferential viscous heating of the ions is also predicted as well as a 10-16 km/sec coronal velocity field.

# RESONANT ELECTRODYNAMIC HEATING OF STELLAR CORONAL LOOPS: AN LRC CIRCUIT ANALOGUE

## I. Introduction

One of the most outstanding problems faced by solar and stellar physicists is an understanding of the cause and effect relationship between inner (e.g., photospheric) and outer (e.g., coronal) atmospheric dynamics. Central to this problem of global coupling within a stellar atmosphere is the role played by magnetic fields. Magnetic fields typically thread the inner and outer atmospheres of a star and thus one cannot disregard the potentially important role that associated electrodynamic processes could play in effecting an "electrodynamic coupling" of these two regions.

A useful parameter that identifies the dominance of "electrodynamic coupling" over, for example, mechanical coupling of the inner and outer atmosphere by acoustic waves, is the plasma beta, $\beta \equiv v_s^2/v_A^2$ ($v_s \equiv$ sound speed; $v_A \equiv$ Alfven speed). Specifically, electrodynamic coupling within a stellar atmosphere dominates mechanical coupling whenever the plasma beta is less than unity within the outer atmosphere, i.e., $\beta_{outer} < 1$, and of the order of unity within the inner atmosphere, i.e., $\beta_{inner} \gtrsim 1$. Thus, mechanical dynamics such as convective and/or differential-rotation velocity fields within the $\beta_{inner} \gtrsim 1$ atmosphere can couple to and drive casually related phenomena, such as heating, within the $\beta_{outer} < 1$ outer atmosphere through various electrodynamic processes associated with the interconnecting magnetic field. This is in contrast to a mechanically coupled stellar atmosphere which would require a $\beta \gtrsim 1$ outer atmosphere.

It is now widely believed that the $\beta \geq 1$ inner (photosphere) and $\beta < 1$ outer (corona) atmosphere of the Sun are electrodynamically coupled since extrapolations of the observed photospheric magnetic energy into the corona exceeds the in-situ thermodynamic energy (i.e., $\beta < 1$). Furthermore, it appears that the solar corona is typically structured, comprising a variety of closed, loop-like regions of enhanced radiative output, i.e., coronal loops (c.f., Withbroe and Noyes, 1977; Vaiana and Rosner, 1978). In this article I will focus upon the electrodynamic coupling of solar coronal loops to their underlying driver -- the $\beta \geq 1$ photospheric velocity field. However, this by no means restricts the applicability of the following analysis to the solar setting. Indeed, the results of this article are generally applicable to any stellar atmosphere and for that matter any cosmic plasma that satisfies the conditions on the plasma $\beta$ as described above.

The specific goals of this article are to:

(i) Determine both the resistive response (i.e., an electrodynamic heating function, $E_H$) and the reactive response (i.e., the induced currents and velocity fields) of magnetic loops in terms of the spectral power of an underlying $\beta \geq 1$ velocity field such as the solar photosphere.

(ii) Utilize the heating function, $E_H$, in an energy balance model which yields the resulting thermal state (i.e., maximum temperature and base pressure) of a loop, also in terms of the spectral power of the $\beta \geq 1$ velocity field.

With regard to (i), there have been a number of attempts at developing a coronal heating function, $E_H$ (c.f., reviews by Wentzel, 1978; Hollweg,1979 ; Kuperus, Ionson and Spicer, 1981). For example the solar physics community has proposed heating by Alfven waves, fast waves, slow waves, Alfvenic surface waves, electrical currents, magnetic reconnection -- a seemingly endless list of possibilities. Unfortunately, there is a very serious problem which appears to be rapidly spreading throughout the solar and into the stellar communities. This problem is associated with the fact that each of the above mentioned mechaniams are being thought of as unique in their own right. This, however, is simply not true since they are all based upon a unifying foundation of electrodynamics whose principle ingredients are capacitance -- the ability of a magnetoplasma to store electric and kinetic energy, inductance -- the ability to store magnetic energy, and resistance -- the ability to convert the above electrodynamic energy into thermodynamic end products such as heat. Another more practical problem with the plethora of proposed heating mechanisms is that they do not result in a heating function which is explicitly correlated with the properties of the $\beta \geq 1$ driver of the corona, viz., the underlying photospheric velocity field. Thus, it has been virtually impossible to develop a complete thermodynamic model that allows us to appreciate coronal loop heating in terms of synchronously observed mechanical activity within the photosphere.

Although some authors have invoked electrodynamic circuit analogues in an attempt to consolidate the many different aspects of electrodynamics into a simple formalism, their approach has for the most part been somewhat too phenomenological as well as limited in scope. Specifically, they have primarily

addressed flare problems in terms of transient $L/R_{Joule}$ discharges (c.f., Alfven, 1977 and references therein). They have not, however, considered continuously driven systems and have also virtually disregarded the critically important capacitive properties of the magnetoplasma, Thus, although their basic phenomenological treatment deserves commendation, the concept of electrodynamic circuit analogues should be rationalized by a more complete and self-consistent treatment. Therefore, upon investigating the important global cause and effect relationship between a coronal loop and its $\beta \geq 1$ driver, one should keep in mind the possibility that the electrodynamics of such a system can be represented by a simple yet *equivalent* driven "LRC" circuit. If this is the case, then a powerful approach to the complex problem of "electrodynamic coupling" in astrophysical plasmas would be at hand since the electrodynamics of simple LRC circuits is well understood. Of course, the key is in the determination of the equivalent L, R, and C values which, as we shall see, is relatively simple to do.

## II. The Physics of Global Electrodynamic Coupling

Figure 1 illustrates both the prototype physical system that will be investigated and its equivalent electrodynamic circuit which will be derived below. The physical system comprises both a $\beta < 1$ magnetic loop and an underlying region of $\beta \geq 1$ velocity fields which electrodynamically couple to and drive electrodynamic activity within the $\beta < 1$ loop via the interconnecting magnetic field $\underset{\sim}{B}_o$. The magnetic loop contains plasma at both coronal and chromospheric temperatures, the transition occurring along the externally

FIG 1

# MAGNETIC LOOP SYSTEM AND EQUIVALENT "LRC" CIRCUIT

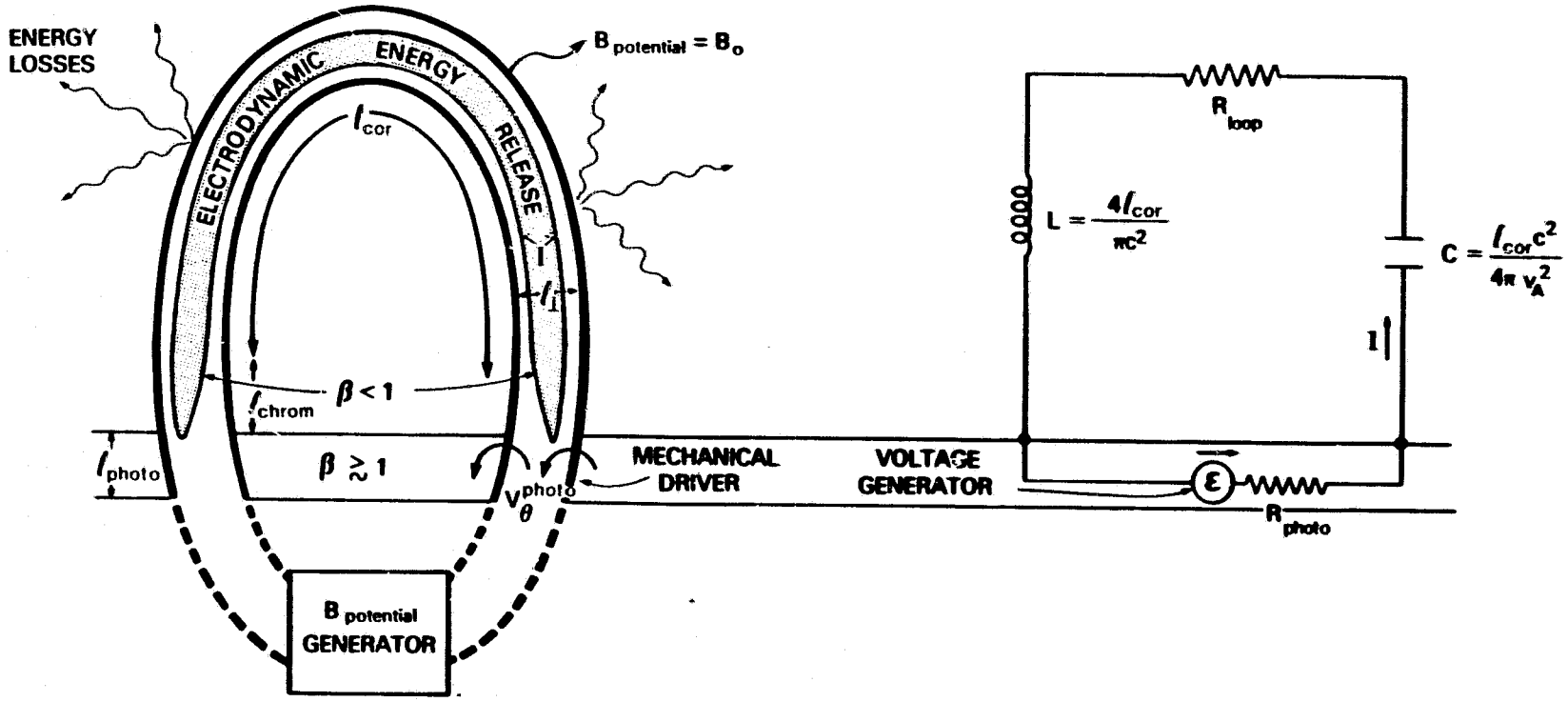

generated potential magnetic field, $\underset{\sim}{B}_o$. The field-aligned scale length of the coronal portion of the magnetic loop will be denoted as $\ell_{cor}$, while the scale length of the chromospheric portion will be denoted as $\ell_{chrom}$. In addition, the field-aligned scale length of the $\beta \geq 1$, photospheric velocity fields which interact with the magnetic loop will be denoted by $\ell_{photo}$. The cross-field scale size of system will be denoted as $\ell_\perp$ which represents the diameter of the magnetic loop in the corona, chromosphere and photosphere. For simplicity $\ell_\perp$ will be assumed to be the same in all three regions -- an assumption that will not adversely affect the analysis presented in this article.

The main field $\underset{\sim}{B}_o$ is generated by a primary dynamo that is external to the loop's local mechanical driver. This is probably the case for many stellar coronal loops in which large scale velocity whose characteristic time scale exceeds the loop's Alfven transit time, are responsible for the overall potential magnetic field structure. It is the relatively smaller scale $\beta \geq 1$ velocity fields, whose characteristic time scale is of the order of the loop's Alfven transit time, which drive the loop into a non-equilibrium electrodynamic state resulting in the flow of electrical currents along (i.e., force-free) and across (i.e., non-forcefree) the ambient field $\underset{\sim}{B}_o$. The equivalent LRC circuit is illustrated in hindsight from the derivation to follow and models the electrodynamic behavior of the physical system. Specifically, the $\beta \geq 1$ velocity fields act as a secondary voltage generator, supplying a time dependent emf, $\mathcal{E}$, which drives an equivalent current, I, though an equivalent loop inductance, L, resistance, $R_{loop}$, and capacitance, C, as well as through an equivalent photospheric resistance, $R_{photo}$.

*(a) Derivation of the Global Electrodynamics Equation*

Magnetohydrodynamic systems are inherently nonlinear. However, experience in handling such complex systems has shown that critically important characteristics become apparent by appropriate linearization. In this regard, the following equations will be linearized with nonlinear modifications being considered later in the article:

$$\frac{4\pi}{c^2}\frac{\partial \underset{\sim}{j}}{\partial t} = -\underset{\sim}{\nabla} \times (\underset{\sim}{\nabla} \times \underset{\sim}{E}) \tag{1}$$

$$\underset{\sim}{\nabla} \cdot \underset{\sim}{j} = 0 \tag{2}$$

$$E + \frac{\underset{\sim}{v} \times \underset{\sim}{B}}{c} = \eta \underset{\sim}{j} \tag{3}$$

$$\rho \frac{\partial \underset{\sim}{v}}{\partial t} + \rho \underset{\sim}{v} \cdot \underset{\sim}{\nabla v} = -\underset{\sim}{\nabla} \cdot \underset{\approx}{P} + \rho \underset{\sim}{g} + \frac{\underset{\sim}{j} \times \underset{\sim}{B}}{c} \tag{4}$$

where

$$\underset{\approx}{P} = p \underset{\approx}{I} - \underset{\approx}{\tau} \tag{5}$$

$$\underset{\approx}{\tau} = \underset{\approx}{\mu} \cdot \underset{\sim}{\nabla} \underset{\sim}{v} \tag{6}$$

$$\mu_\perp = \rho \rho_{ci}^2 \nu_i / (1 + \nu_i^2/\Omega_i^2) \tag{7}$$

$$\mu_\parallel = \mu_\perp (1 + \Omega_i^2/\nu_i^2) \tag{8}$$

$$\eta = \frac{4\pi \nu_e}{\omega_{pe}^2} \tag{9}$$

and where the electron collision frequency, $\nu_e$, and ion collision frequency, $\nu_i$, are given by:

$$\nu_e = \nu_{e\text{-}i} + \nu_{e\text{-neutral}} + \nu_{anomalous} \tag{10}$$

$$\nu_i \cong (m_e/m_i)^{1/2}\ \nu_e \text{ for } T_e \sim T_i, \tag{11}$$

with the electron-ion collision frequency, $\nu_{e\text{-}i}$, given by:

$$\nu_{e\text{-}i} \cong 50.0\ (n_e/T_e^{3/2})\ \text{sec}^{-1}, \tag{12}$$

the electron-neutral collision frequency, $\nu_{e\text{-}n}$ given by:

$$\nu_{e\text{-}n} \cong 1.95 \times 10^{-9}\ n_n\ T_e^{1/2}\ \text{sec}^{-1} \tag{13}$$

and with the anomalous collision frequency, $\nu_{anomalous}$, of electrons with a non-thermal level of low frequency ($\omega \leq \omega_{pi}$) electrostatic plasma waves being given by:

$$\nu_{anomalous} \cong \omega_{pe} \left(\frac{W}{n_e k_B T_e}\right) \leq \omega_{pi} \tag{14}$$

where W is the energy density of the plasma microturbulence. Such plasma microturbulence could develop if the electrical currents exceed various threshold conditions (c.f., Papadopoulos, 1977; Ionson et al., 1979; Rosner et al., 1978; Hinata, 1980).

The electrodynamics equation (1) is given in terms of the local current density, $\underset{\sim}{j}$, and electric field, $\underset{\sim}{E}$. In analyzing this equation I will adopt a cylindrical coordinate system in which $\hat{x}_{\|}$ represents a direction parallel to

the ambient field, $\underset{\sim}{B}_o$, and in which $\hat{x}_\perp$ represents a direction perpendicular to the field. The perpendicular unit vector, $\hat{x}_\perp$, contains two bases, viz., $\hat{x}_\theta$ which corresponds to the azimuthal direction and $\hat{x}_r$ which corresponds to the radial direction. In addition, variations in plasma parameters such as the Alfven speed will occur only in the $\hat{x}_\parallel$ and $\hat{x}_r$ directions.

In order that the Poynting flux be directed primarily along the ambient field, $\underset{\sim}{B}_o$, it follows that $(\underset{\sim}{\nabla} \times \underset{\sim}{E})_\parallel \sim 0$ (i.e., approximately shear disturbances). Note that the field aligned perturbation in the magnetic field is not identically zero thereby resulting in a small component of the Poynting flux in the $\hat{x}_\perp$ direction. This is important since it allows the "interior" of a coronal loop to receive electrodynamic energy from "exterior" regions of a loop. Note also that the condition $(\underset{\sim}{\nabla} \times \underset{\sim}{E})_\parallel \sim 0$ is equivalent to disturbances that are approximately incompressible (i.e., $\underset{\sim}{\nabla} \cdot \underset{\sim}{v} \sim 0$) thereby rationalizing the use of an incompressible momentum equation (4). Although nonlinearities could convert shear into compressible disturbances therefore requiring use of a compressible momentum equation (Hollweg, 1981), it is important to first consider the linearized, shear system. In section II.(e), I will briefly discuss some simple nonlinear modifications of the linear analysis.

Under the constraint that $(\underset{\sim}{\nabla} \times \underset{\sim}{E})_\parallel \sim 0$ it follows that $\underset{\sim}{\nabla}_\perp (\underset{\sim}{\nabla}_\perp \cdot \underset{\sim}{E}_\perp) - \nabla_\perp^2 \underset{\sim}{E}_\perp \sim 0$ and thus equation (1) can be written in the following component form:

$$\frac{4\pi}{c^2} \frac{\partial j_\parallel}{\partial t} + \frac{\partial}{\partial x_\parallel} (\underset{\sim}{\nabla}_\perp \cdot \underset{\sim}{E}_\perp) - \underset{\sim}{\nabla}_\perp^2 E_\parallel = 0 \qquad (15)$$

$$\frac{4\pi}{c^2}\frac{\partial \underset{\sim}{j}_{\perp}}{\partial t} + \underset{\sim}{\nabla}_{\perp}\left(\frac{\partial E_{||}}{\partial x_{||}}\right) - \frac{\partial^2 \underset{\sim}{E}_{\perp}}{\partial x_{||}^2} = 0 \qquad (16)$$

Noting in hindsight that $\partial/\partial x_r \gg \partial/\partial x_\theta$ due to a local resonance absorption process that will be discussed later, it follows that $E_\theta \ll E_r$; and since $\underset{\sim}{j}_{\perp} \propto \dot{\underset{\sim}{E}}_{\perp}$ the $\underset{\sim}{j}_{\perp}$ current is carried primarily by $j_r$. Using Ohm's law (i.e., equation (3)) the electrodynamics is therefore described by,

$$\frac{4\pi}{c^2}\frac{\partial^2 j_r}{\partial t^2} + \frac{\partial^2}{\partial x_r \partial x_{||}}\left(\eta \frac{\partial j_{||}}{\partial t}\right) - \frac{\partial^2}{\partial x_{||}^2}\left(\eta \frac{\partial j_r}{\partial t}\right) + \frac{1}{c}\frac{\partial^3 (v_\theta B)}{\partial x_{||}^2 \partial t} = 0 \qquad (17)$$

$$\frac{4\pi}{c^2}\frac{\partial^2 j_{||}}{\partial t^2} + \frac{\partial^2}{\partial x_r \partial x_{||}}\left(\eta \frac{\partial j_r}{\partial t}\right) - \underset{\sim}{\nabla}_{\perp}^2\left(\eta \frac{\partial j_{||}}{\partial t}\right) - \frac{1}{c}\frac{\partial^3 (v_\theta B)}{\partial x_{||} \partial x_r \partial t} = 0 \qquad (18)$$

Since $\underset{\sim}{\nabla} \cdot \underset{\sim}{j} = 0$ (i.e., $\partial j_r/\partial x_r = -\partial j_{||}/\partial x_{||}$), equations (17) and (18) are redundant. This redundancy is primarily a consequence of the $(\underset{\sim}{\nabla} \times \underset{\sim}{E})_{||} \sim 0$ constraint. Thus it is necessary to consider only one of the above equations since they both contain a complete electrodynamic description. In this regard I will focus upon equation (18), rewritten in the following form.

$$\frac{4\pi}{c^2}\frac{\partial^2 j_{||}}{\partial t^2} - \frac{\partial^2}{\partial x_r^2}\left(\eta \frac{\partial j_{||}}{\partial t}\right) - H(1-\beta)\frac{\partial^3 (v_\theta B_o/c)}{\partial x_{||} \partial x_r \partial t} = H(\beta-1)\frac{\partial^3 (v_\theta B/c)}{\partial x_{||} \partial x_r \partial t} \qquad (19)$$

where $H(1-\beta)$ is the Heavyside step function and with $\beta$ as the plasma beta (i.e., $H(1-\beta) = 0$ for $\beta > 1$ and $= 1$ for $\beta < 1$) and where the second term on the left hand side of equation (18) has been neglected since it is small compared to the other terms.

The third term on the left hand side of equation (19) contributes only in $\beta < 1$ regions and represents the hydrodynamic reactance of the plasma to externally applied emfs associated with the $\beta \gtrsim 1$ velocity fields (i.e., the right hand side of equation (19)). The $\beta < 1$ reactance term can readily be determined via the force balance equation (4) valid in $\beta < 1$ regions, i.e.,

$$\rho \frac{\partial \underset{\sim}{v}_\perp}{\partial t} \equiv \frac{\underset{\sim}{j} \times \underset{\sim}{B}_o}{c} + \mu_\perp \nabla_\perp^2 \underset{\sim}{v}_\perp . \tag{20}$$

Using the correspondence $\partial/\partial t \rightarrow i\omega$ and noting in hindsight that the reactance is maximum when $\partial/\partial t \sim v_A \partial/\partial x_\parallel$, it follows that

$$\frac{\partial^3 (v_\theta B_o/c)}{\partial x_\parallel \partial x_r \partial t} \simeq Pr_{mag}\, \eta \frac{\partial j_\parallel^3}{\partial x_r^2 \partial t} + \frac{4\pi v_A^2}{c^2} \frac{\partial^2 j_\parallel}{\partial x_\parallel^2} \tag{21}$$

where the magnetic Prandtl number $Pr_{mag}$ is defined as the ratio of momentum diffusion to magnetic diffusion, i.e.,

$$Pr_{mag} \equiv \frac{4\pi\mu_\perp}{\rho c^2 \eta} \simeq \beta \left(\frac{m_i}{m_e}\right)^{1/2} \left(1 + \frac{\nu_i^2}{\Omega_i^2}\right)^{-1} . \tag{22}$$

Using equation (21), the local electrodynamics equation (19) reduces to,

$$\frac{4\pi}{c^2} \frac{\partial^2 j_\parallel}{\partial t^2} - \eta \left(1 + H(1-\beta) Pr_{mag}\right) \frac{\partial^2 j_\parallel}{\partial x_r^2 \partial t} - H(1-\beta) \left(\frac{4\pi v_A^2}{c^2}\right) \frac{\partial j_\parallel^2}{\partial x_\parallel^2} = H(\beta-1) \frac{\partial^3 (v_\theta B_o/c)}{\partial x_\parallel \partial x_r \partial t} \tag{23}$$

and one begins to see the emergence of a simple "LRC" circuit analogue -- the first term representing an inductive reactance, the second term representing a Joule and viscous resistance, the third term representing a capactive reactance and the term on the right hand side representing the external source of emf which drives the currents.

Equation (23) describes the local electrodynamics of the system. A description of the global electrodynamics is obtained by integrating equation (23) over the volume of the system. In performing this integration it is important to note the possible occurrence of a local resonance absorption process in the $\beta \ll 1$ magnetic loop. This process has been discussed in some detail by a number of authors (e.g., Hasegawa and Chen, 1976; Kappraff and Tataronis, 1977; Ionson, 1977, 1978, 1981; Ott et al., 1979). Although most of these discussions are strictly applicable for specific plasma parameters (e.g., collisionless or collisional analyses), Ionson (1981) has presented the concept in a relatively unified manner which I will briefly review for the case of a collisional plasma (i.e., the electron pressure $\underset{\sim}{E}$-field which supports kinetic Alfven waves is small compared to the resistive $\underset{\sim}{E}$-field).

Noting that there is a cross-field variation in the Alfven speed, $dv_A/dx_r$, it follows that for a particular driving frequency, $\omega$, absorption of electrodynamic energy could occur within a small spatial bandwidth, $\Delta x_r$, centered about a spatial resonance located at $x_r = x_{res}$. For a specific $x_{||}$, a spatial resonance exists only if $v_A(x_r = x_{res})\partial/\partial x \neq \omega$ at some point in the $\hat{x}_r$-direction--a condition that is not necessarily satisfied. However, if this resonance condition is satisfied, the spatial bandwidth, $\Delta x_r$, can readily be estimated from equation (23) by expanding the Alfven speed about the spatial resonance and

noting that the inductive and capacitive reactances cancel one another at the spatial resonance, $x_r = x_{res}$, i.e., $4\pi\partial^2 j_{||}/c^2\partial t^2 \cong 4\pi v_A^2(x_{res})\partial^2 j_{||}/\partial x_{||}^2$. A consequence of matching the inner resistive solution to the outer reactive solution (i.e., the ideal mhd solution) is that the resistive term in equation (23) equals the first order contribution of the expanded capacitive term, i.e.,

$$\frac{\eta(1 + Pr_{mag}\, H(1-\beta))\ \omega\, \pi^2}{(\Delta x_r)^2} = \frac{4\pi\ \omega^2\ (\Delta x_r)}{ac^2} \tag{24}$$

where

$$a \equiv \left(\frac{d(\ell n\ v_A)}{dx_r}\right)^{-1} \tag{25}$$

and where the correspondence $\partial/\partial x_r \rightarrow i\pi/(\Delta x_r)$ has been used. Solving equation (24) for $\Delta x_r$ yields,

$$\frac{\Delta x_r}{\ell_\perp} = \pi^{1/3}\left(\frac{a}{\ell_\perp}\right)^{1/3} (1 + Pr_{mag}\, H(1-\beta))^{1/3}\ Re_{mag}^{-1/3} \tag{26}$$

where the magnetic Reynold's number, $Re_{mag}$, is defined as,

$$Re_{mag} \equiv \frac{4\pi\ v_A^{local}\ \ell_\perp^{\,2}}{\eta\, c^2 \ell_{||}}\,. \tag{27}$$

where $\partial/\partial x_{||} \rightarrow i\pi/\ell_{||}$ has been used with $\ell_{||}$ representing the field-aligned extent of the local region. It should be noted that $\Delta x_r$ as defined by equation (26) depends upon local plasma parameters such as the resistivity, $\eta$, Alfven speed,

$v_A^{local}$, the magnetic Prandtl number, $Pr_{mag}$ and the field-aligned extent of the local region, $\ell_{||}$. It is also important to note that equation (26) implicitly assumes the existence of a spatial resonance.

Keeping in mind that $\Delta x_r$ can be interpreted as the local (i.e., along the magnetic field), characteristic cross-field shear length of the induced current and velocity fields, equation (23) can be simply integrated over the volume of the system. This results in a description of the system's global electrodynamics which is represented by the following global electrodynamics equation:

$$L \frac{d^2 I}{dt^2} + R_{global} \frac{dI}{dt} + \frac{I}{C} = \frac{d\mathcal{E}(t)}{dt} \tag{28}$$

where the equivalent inductance, L, capacitance, C, resistance, $R_{global}$, current, I, and driving emf, $\mathcal{E}(t)$ are given by,

$$L = \frac{4\bar{\ell}_{||}}{\pi c^2} \tag{29}$$

$$C = \frac{\bar{\ell}_{||} c^2}{4\pi \bar{v}_A^2} \tag{30}$$

$$R_{global} = R_{loop} + R_{photo} \tag{31}$$

$$R_{loop} = \sum_{\substack{\text{chromosphere} \\ \text{corona}}} \eta (1 + Pr_{mag}) \ell_{||}/(\Delta x_r)^2 \tag{32}$$

$$R_{photo} = \frac{\eta_{photo} \ell_{photo}}{(\Delta x_r)^2_{photo}} \tag{33}$$

$$I = \pi \ell_{\perp} (\Delta x_r)\, j_{\parallel} = \pi \ell_{\perp} \ell_{\parallel} j_r \tag{34}$$

$$\mathcal{E}(t) = \left( \frac{\ell_{\perp} v_{\theta} B}{c} \right)_{\text{photo}} . \tag{35}$$

(b) *Discussion of an Electrodynamic Circuit Analogue*

It's clear from equation (28) that the global electrodynamics of the magnetic loop system can be modelled via a simple LRC circuit analogue. The equivalent circuit elements described by equations (29)-(33) obviously represent averages over the loop and its underlying mechanical driver. Specifically, $\bar{\ell}_{\parallel}$ and $\bar{v}_A$ found in equations (29) and (30) represent a characteristic length of the system and a characteristic average value for the Alfven speed whose explicit dependence upon spatial details of the system is at this stage not overly important. In fact, since the majority of the system resides within the corona where the Alfven speed is at its maximum value, the expressions for the inductance and capacitance can for all practical purposes be written as,

$$L = \frac{4\ell_{cor}}{\pi c^2} \tag{36}$$

$$C = \frac{\ell_{cor} c^2}{4\pi v_A^2} \tag{37}$$

where it is understood that $v_A$ refers to the coronal Alfven speed. An important point to be made here is that the magnetic loop naturally supports global structure oscillations at a characteristic frequency, $\omega_o$, given by,

$$\omega_o = \frac{1}{\sqrt{L\,C}} = \frac{\pi v_A}{\ell_{cor}} \tag{38}$$

One such example of global structure oscillations which are characterized by high shear are Alfvenic "surface" waves (c.f., Ionson, 1977, 1978; Wentzel, 1979, and references within these articles). It is important to note that Alfvenic "surface" waves *do not* require a discontinuous Alfven speed profile. In fact, any degree of nonuniformity will support their existence. Hollweg (1981) has also stressed the importance of global loop resonances. Thus it appears that the formalism presented in this article casts the concept of *global* structure oscillations and resonances into a unified picture. That is, according to the derived electrodynamic circuit analogue, these global oscillations can be interpreted as global LC oscillations. Of course, this point was missed by previous proponents of electrodynamic circuit analogues since they, in their purely phenomenological treatment, did not account for a critically important energy storage element -- the capacitance. The capacitance is important because it describes the hydrodynamic reactance of the plasma to imposed emfs, an essential feature of all hydromagnetic oscillations. This can be simply understood by noting that the energy stored by the capacitor is $1/2\ C\ \Phi^2$ where $C = C_o K$ (the free space capacitance across field lines being $C_o = \ell_{\parallel}/4\pi$ and $K$ being the plasma dielectric) and where $\Phi \tilde{=} \ell_\perp E_\perp$ is the average electric potential across the field lines. Since the low-frequency dielectric $K \tilde{=} 1 + c^2/v_A^2$, one can see immediately that the energy stored by the capacitor comprises two parts, viz., the electric field energy per unit volume, $E_\perp^2/8\pi$ and the polarization energy per unit volume, $c^2E_\perp^2/8\pi v_A^2$. Noting that $v_\perp \approx cE_\perp/B_o$,

the polarization energy is therefore in the form of kinetic energy, $1/2\rho v_\perp^2$. In fact, the so-called polarization current $\underset{\sim}{j}_\perp^{pol.}$ is defined such that $\underset{\sim}{j}_\perp^{pol.} \times \underset{\sim}{B}_o/c = \rho \underset{\sim}{v}_\perp$ resulting in $\underset{\sim}{j}_\perp^{pol.} = c^2 \underset{\sim}{\dot{E}}_\perp / 4\pi v_A^2$, which is consistent with a derivation of $\underset{\sim}{j}_\perp^{pol.}$ using particle orbit theory.

Since the hydrodynamic reactance of the $\beta \gtrsim 1$ plasma (i.e., related to C) is associated with electrodynamically-induced velocity fields, one must also self-consistently include viscous dissipation. Therefore, just as Joule dissipation is an importance source of resistance, $R_{Joule}$, to current flow, so is viscous dissipation since it tends to prevent the electrodynamic charging of the $\beta < 1$ plasma capacitor by inhibiting the development of polarization velocity fields within the magnetic loop. Although viscous drag is also important within the $\beta \gtrsim 1$ photospheric driver, it does not explicitly appear in the electrodynamic description of the system. Rather, photospheric viscosity is implicitly included in the driving emf, $\mathcal{E}(t)$, which depends upon the photospheric velocity field, which in turn depends upon a balance of inertial, non-electrodynamic and viscous forces. Within the $\beta < 1$ magnetic loop, however, viscous dissipation makes an explicit showing in an LRC analogue as a phenomenological viscous resistor, $R_{viscous} = Pr_{mag} R_{Joule}$ where the magnetic Prandtl number is defined by eqn. (22) and where the Joule resistance, $R_{Joule} = \eta \ell_{||}/(\Delta x_r)^2$. Therefore, the $\beta < 1$ resistance, $R_{loop}$, given by equation (32) is the sum of $R_{Joule}$ and $R_{viscous}$ over both the chromosphere and corona. Note that the plasma parameters found within the summation of equation (32) represent local conditions with $\ell_{||}$ and

$\Delta x_r$ being the field-aligned extent of the region, and the local cross-field shear length of the induced currents and velocity fields which is given by equation (26) if local resonance absorption occurs.

Since the cross-field shear length, $\Delta x_r$, represents the cross-field spatial extent of the field-aligned current, it is clear that the total field-aligned current, $I_{||} = \pi \ell_\perp (\Delta x_r) j_{||}$. It is important to note that $I_{||} \simeq I_r$ -- a consequence of the shear constraint, $(\underset{\sim}{\nabla} \times \underset{\sim}{E})_{||} \sim 0$. Note that $I_r$ cannot possible be zero since it is driven by perpendicular, polarization $E_r$-fields which are essential for the establishment of a non-zero Poynting flux into the loop from its underlying driver. Therefore, even though $j_{||} >> j_r$ seems to indicate that most of the induced current is force-free it must be kept in mind that $j_{||}$ is confined to flow a filament of thickness $\Delta x_r$ whereas $j_r$ flows through a filament of thickness $\ell_\perp >> \Delta x_r$. Therefore the total currents, $I_r = \pi \ell_\perp (\Delta x_r) j_{||}$ and $I_{||} = \pi \ell_\perp \ell_{||} j_r$, are equal as is pointed out in equation (34). It is very important to note that steady heating of magnetic loops from an underlying driver is always associated with Lorentz forces within the loop which induce a $\beta < 1$ velocity field. This effect is a natural consequence of the capacitive term in equation (28).

A simple way that the $\Delta x_r$ can be estimated, which is equivalent to the derivation in section II.a., is to think of the global structure oscillation as an exciter of internal field line oscillations within a spatial bandwidth $\Delta x_r$. In other words, there is a mode coupling between the global structure oscillation and local field line oscillations at that point where $\omega_o = \omega$ with $\omega = \pi v_A(x_r)/\ell_{||}$ being the local eigenfrequency. Noting a correspondence between the width of a local frequency resonance, $\Delta\omega$, and the width of the local spatial resonance, $\Delta x_r$, i.e.,

$$\frac{\Delta\omega}{\omega} \sim \frac{\Delta x_r}{a} \tag{39}$$

where the Alfven speed's gradient scale length, "a" is defined by equation (25). Since the width of a frequency resonance depends upon dissipation through an oscillator's "Q" value, i.e.,

$$\frac{\Delta\omega}{\omega} \simeq \frac{1}{Q} \tag{40}$$

where $Q = \sqrt{L/C}/R$ is the ratio of the oscillator's natural impedence to the resistive impedence, so must the width of a spatial resonance depend upon the magnetic loop system's local "$Q_{local}$" value, i.e.,

$$\frac{\Delta x_r}{a} \simeq \frac{1}{Q_{local}} \tag{41}$$

where

$$Q_{local} = \frac{1}{R_{local}} \left(\sqrt{\frac{L}{C}}\right)_{local} \tag{42}$$

Noting that $R_{local}$ corresponds to the local resistance described by equations (32) and (33), and that the local natural impedence is proportional to the local Alfven speed, equation (42) reduces to,

$$Q_{local} = \Pi^{-1} \left(1 + Pr_{mag}\, H(1-\beta)\right) \left(\frac{\Delta x_r}{\ell_\perp}\right)^2 Re_{mag} \tag{43}$$

where the magnetic Reynold's number, $Re_{mag}$, is defined by equation (27) and where $H(1 - \beta)$ is the Heavyside step function which is used to illustrate that the viscous resistor does not appear in $\beta \geq 1$ regions. Using equation (43) in

equation (41) and solving for $\Delta x_r$ immediately yields equation (26). Therefore, for a specific driving frequency, $\omega_i$ (e.g., a loop's global resonance frequency, $\omega_o$) absorption will occur along resonant field lines of width $\Delta x_r$ given by equation (26), provided the condition for the existence of spatial resonances is satisfied, i.e., $v_A\,(x_r = x_{res})\partial/\partial x_{||} \rightarrow \omega_i$. In this regard, the local resistances, normalized to the natural impedence of the entire magnetic loop system, i.e., $\bar{R}_{local} \equiv R_{local}\sqrt{C/L}$, depend upon the magnetic Reynold's number in two different ways depending upon whether or not local resonance absorption is occurring, viz.,

$$\bar{R}_{local} = \pi(1 + Pr_{mag}\, H(1 - \beta))\left(\frac{v_A^{local}}{v_A}\right) Re_{mag}^{-1};\ \begin{matrix}\text{locally}\\ \text{non-resonant}\end{matrix} \qquad (44)$$

$$R_{local} = \pi^{1/3}\left(\frac{a}{\ell_\perp}\right)^{-2/3}(1 + Pr_{mag}\, H(1 - \beta))^{1/3}\, Re_{mag}^{-1/3};\ \begin{matrix}\text{locally}\\ \text{resonant}\end{matrix} \qquad (45)$$

These normalized resistances are also related to the global quality, $Q_{global}$, of the entire loop system defined as the ratio of the system's natural impedence, $\sqrt{L/C}$, to the total resistance in the circuit, i.e.,

$$Q_{global} \equiv \left[\sum_{\substack{\text{photosphere}\\ \text{chromosphere}\\ \text{corona}}} R_{local}\right]^{-1} \qquad (46)$$

As I have already mentioned, local resonance absorption does not necessarily occur everywhere along the magnetic loop system. However, this process does

occur at least in the coronal portion of the magnetic loop where the local resonance condition is easily satisfied.

It is becoming quite apparent that given the driving emf, $\mathcal{E}(t)$, which is explicitly correlated with the non-electrodynamically driven, $\beta \gtrsim 1$ photospheric velocity field (c.f., equation (35)), it is a simple matter to determine the electrodynamic response of the magnetic loop. This response comprises both a resistive and reactive component. The resistive response is, of course, related to the electrodynamic heating function, $E_H$, which will be derived in the next section. The reactive response is both microscopic as well as macroscopic. The microscopic response is associated with the field-aligned current, $j_{\parallel}$, which is carried primarily by the electron fluid and which, in the context of the one-fluid model used in this article, can be thought of as a microscopic ingredient of the plasma. The macroscopic response is associated with the cross-field polarization current, $j_r$, which is carried primarily by the ion fluid. The polarization current, $j_r$, results in a Lorentz force, $j_r \times B_o/c$, which drives a macroscopic velocity field within the magnetic loop. These reactances will be derived in section II.(d) and will yield very important information regarding the possible development of microscopic nonlinearities such as anomalous transport and macroscopic nonlinearities such as the conversion of sheared flow fields into compressible flow fields.

(c) *The Generalized Electrodynamic Heating Function, $E_H$*

In general, the driving emf, $\mathcal{E}(t)$, in the global electrodynamics equation (28) is best represented as a stationary random variable. This follows from the fact that the $\beta \geq 1$ velocity field, $\underset{\sim}{v}(t)$, which generates the emf, $\mathcal{E}(t)$, is also a stationary random variable. Kolmogoroff proved in 1940 that every stationary random process can be represented by a linear combination of harmonic oscillations. If the duration of the process is very long and we want good accuracy, one must use an increasingly larger number of harmonic oscillations spaced arbitrarily closely. Formally, this is expressed by the Fourier-Stieltjes transform. Specifically, the transform of $\mathcal{E}(t)$ and its inverse are given by

$$\mathcal{E}(t) = \int_{-\infty}^{\infty} e^{i\omega t}\, d\mathcal{E}_\omega \tag{47}$$

with

$$\mathcal{E}_\omega = \lim_{t\to\infty} \left(\frac{1}{2\pi}\right) \int_{-t}^{t} \frac{1 - e^{-i\omega t}}{it}\, \mathcal{E}(t)dt. \tag{48}$$

We can readily appreciate that $d\mathcal{E}_\omega$ are like Fourier coefficients but in this representation discontinuous jumps in $\mathcal{E}_\omega$ are allowed. This formalism therefore permits analysis of random variables which contain discrete frequencies superimposed upon a continuous spectrum, a common situation in turbulent systems such as the solar convection zone. Furthermore, since we are dealing with stationary random processes, it follows that the ensemble average of $\mathcal{E}(t)$ and $d\mathcal{E}_\omega$ are both zero, i.e.,

$$\langle \mathcal{E}(t) \rangle = \langle d\mathcal{E}_\omega \rangle = 0 \tag{49}$$

where the brackets represent an ensemble average. Since the ensemble average of products of random variables are in general non-zero, they are physically significant. Specifically, the spectral "power" $\langle d\mathcal{E}^2 \rangle_\omega$ is represented by

$$\langle d\mathcal{E}^2 \rangle_\omega = (d\mathcal{E}^*_\omega \, d\mathcal{E}_\omega) = \langle \mathcal{E}^2 \rangle_\omega \, d\omega \tag{50}$$

and is related to $\langle \mathcal{E}^*(t)\mathcal{E}(t) \rangle$ via

$$\langle \mathcal{E}^*(t)\mathcal{E}(t) \rangle = \int_{-\infty}^{\infty} \langle d\mathcal{E}^2 \rangle_\omega \tag{51}$$

where the * refers to the complex conjugate.

Armed with this powerful formalism, it is a simple matter to determine the generalized electrodynamic heating function, $E_H$ which is defined by,

$$E_H = \frac{4}{\pi \ell_\perp^2 \ell_{cor}} < I^*(t) I(t) R_{loop} > \tag{52}$$

where $\pi \ell_\perp^2 \ell_{cor}/4$ is the volume of the coronal loop and where $R_{loop}$ is defined by equation (32) which is evaluated by using either equation (44) or (45). Taking the Fourier-Stieltjes transform of equation (28) yields,

$$I_\omega = \frac{\mathcal{E}_\omega}{R_{global} \left[1 + i(\omega/\omega_o - \omega_o/\omega) Q_{global}\right]} \tag{53}$$

where $R_{global}$ and $Q_{global}$ are defined by equations (31) and (46). Noting that

$$< I^*(t)I(t) > = \int_{-\infty}^{\infty} < dI_\omega^* \, dI_\omega > \tag{54}$$

and using this expression along with equation (52) results in a generalized electrodynamic heating function which is given by,

$$E_H = \frac{4}{\pi \ell_\perp^2 \ell_{cor}} \int_{-\infty}^{\infty} \frac{<\mathcal{E}^2>_\omega R_{loop}}{R_{global}^2} p_f(\omega) d\omega \tag{55}$$

where the "power factor," $p_f(\omega)$ is given by,

$$p_f(\omega) = \frac{1}{[1 + (\omega/\omega_o - \omega_o/\omega)^2 Q_{global}^2]} \tag{56}$$

The well known plot of $p_f(\omega)$ versus $\omega/\omega_o$ is illustrated in Figure 2. Clearly, for $Q_{global} \gg 1$ the power factor is sharply peaked about $\omega = \omega_o$. We shall see that magnetic loops typically have $Q_{global} \gg 1$ allowing a simple evaluation of the integral in equation (55). Specifically, $<\mathcal{E}^2>_\omega$ can be taken outside the integral provided it is evaluated at the resonance frequency $\omega = \omega_o$. It is then a simple matter to evaluate the integral of the power function over frequency, resulting in a resonant electrodynamic heating given by,

$$E_H = \left(\frac{4}{\pi \ell_\perp^2 \ell_{cor}}\right) \left(\frac{\langle \mathcal{E}^2 \rangle_{\nu_o} \pi \nu_o}{Q_{global}}\right) \left(\frac{R_{loop}}{R_{global}^2}\right) . \tag{57}$$

FIG 2

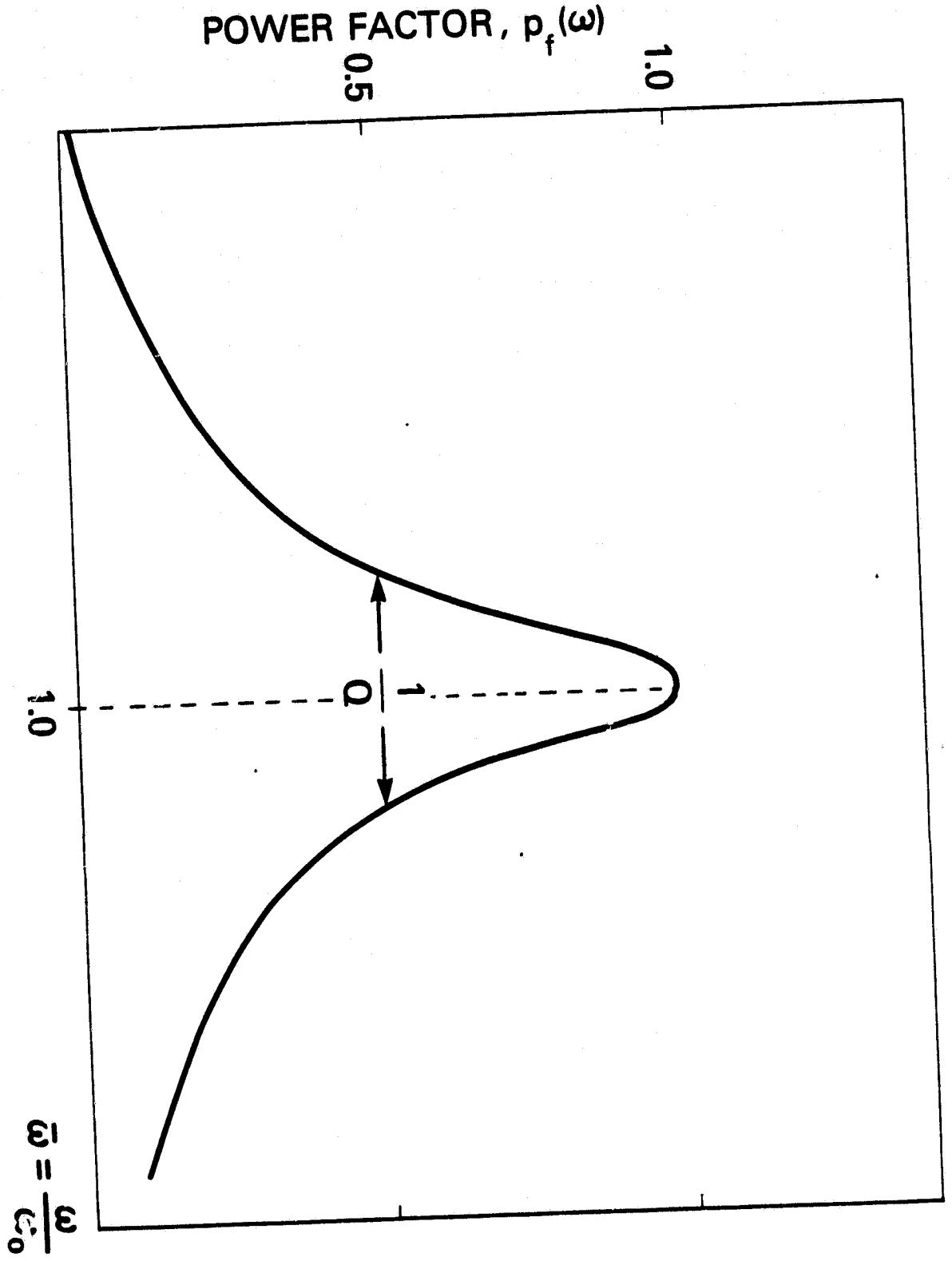

where $\omega_o = 2\pi\nu_o$ has been used. Eliminating $Q_{global} = \sqrt{L/C}/R_{global}$ from equation (57) yields a result that is virtually independent of dissipation, i.e.,

$$E_H = \left(\frac{4}{\pi \ell_\perp^2 \ell_{cor}}\right)\left(\frac{<\mathcal{E}^2>_{\nu_o} \pi \nu_o}{\sqrt{L/C}}\right)\left(\frac{R_{loop}}{R_{global}}\right). \qquad (58)$$

In fact, the power drain on the driver, $E_H R_{global}/R_{loop}$, is apparently totally independent of dissipation. *This is a classic feature of resonance phenomena and does not imply that irreversibilities are unimportant.* Irreversibilities determine the fraction $\Delta\nu_o/\nu_o = \pi/Q_{global}$, of the available driving emf, $<\mathcal{E}^2>_{\nu_o} \nu_o$, that interacts with the electrodynamic system at resonance. Since at resonance the inductive and capacitive impedences cancel one another, the total power drain on the driver equals $<\mathcal{E}^2>_{\nu_o} \Delta\nu_o/R_{global}$ which is explicitly independent of the dissipation since $\Delta\nu_o \propto R_{global}$. Of course, the power absorbed by the loop is simply $R_{loop}/R_{global}$ times the power drain on the driver (i.e., c.f., equation (58)).

An important point to note regarding equation (58) is that resonant heating of magnetic loops is characterized by an explicit correlation between the spectral details of the $\beta \gtrsim 1$ velocity field and the power absorbed by the loop which, of course, critically participates in determining the loop's thermodynamic state. Noting that

$$<\mathcal{E}^2>_{\nu_o} \simeq 16\pi (v_A^{photo} \ell_\perp/c)^2 \quad <1/2\ \rho v_\theta^{2\,photo}>_{\nu_o} \qquad (59)$$

which includes a factor of two stemming from the fact that there are two sources of emf, one at each footpoint, equation (58) can be rewritten as

$$E_H = 16\pi \left(\frac{v_A^{photo}}{v_A}\right)\left(\frac{v_A^{photo}}{\ell_{cor}}\right)\left(\frac{R_{loop}}{R_{global}}\right) < 1/2\ \rho v_\theta^2 >^{photo}_{\nu_o} \nu_o \qquad (60)$$

In the context of the above discussion, this result can easily be derived from ideal mhd, noting that all electrodynamic energy entering the loop will be in reality dissipated -- a point stressed by Ionson (1977, 1978) who argues in favor of an underdamped, high-quality resonant system with $Q_{global} \gg 1$; and also stressed by Rosner et al. (1978) and Golub et al. (1980) who argue in favor of an overdamped, low quality system with $Q_{global} < 1$. Specifically, the net flux of energy into a loop is the product of the transmittance, $2v_A^{photo}/v_A$, the input signal speed, $v_A^{photo}$, the energy density of the $\beta \geq 1$ photospheric velocity field, $< 1/2\ \rho v_\theta^2 >^{photo}_{\nu_o} \nu_o$, the number of polarization states which equals two for electrodynamic disturbances, the number of normal modes which equals two for low-frequency electrodynamic disturbances in $\beta < 1$ plasmas, the number of sources which equals two for a magnetic loop with two footpoints, and the fractional dissipation within the loop, $R_{loop}/R_{global}$. Noting also that the power absorbed per unit volume is the divergence of the above product of terms with $\nabla \sim \pi/\ell_{cor}$, one readily recovers the generalized electrodynamic heating function, $E_H$, given by equation (60). Since $v_A^{photo} \simeq v_{sound}^{photo} = \sqrt{3k_B T_{eff}/m_i}$ where $T_{eff}$ is the effective black-body temperature of the star, the heating function can also be written as,

$$E_H = 6.28 \times 10^9 \left(\frac{T_{eff}}{\ell_{cor}^2}\right)\left(\frac{R_{loop}}{R_{global}}\right) < 1/2\ \rho v_\theta^2 >^{photo}_{\nu_o} \left(\frac{ergs}{cm^3\text{-}sec}\right) \qquad (61)$$

Equations (60) or (61) are of major importance since they clearly reveal how the electrodynamic heating function scales with the spectral power of the $\beta \gtrsim 1$ photospheric velocity field (i.e., goal (i) of the Introduction). The essential feature of a resonant heating mechanism is that magnetic loops with different lengths, and hence different global resonance frequencies, $\nu_o = v_A/2\ell_{cor}$, are heated at a rate that critically depends upon the amount of $\beta \gtrsim 1$ spectral power found at $\nu_o$, viz., $< 1/2\ \rho v_\theta^2 >^{photo}_{\nu_o}$. This is in complete contrast to a non-resonant heating mechanism (i.e., $Q_{global} < 1$) which would depend upon the total power (i.e., the spectral power summed over all frequencies) rather than the details of the photospheric velocity field's spectral power function. Thus, although all electrodynamic energy entering the magnetic loop would be immediately dissipated by a non-resonant heating mechanism, as has been pointed out by Rosner et al. (1978) and Golub et al. (1980) there would be no correlation between the amount of energy absorbed by a loop of length $\ell_{cor}$ (and hence its temperature and pressure) and the photospheric spectral power at $\nu_o = v_A/2\ell_{cor}$. Note also that although the role of the magnetic field, $B_o$, appears to be passive for a resonant heating mechanism, in the sense that it participates in determining a loop's global resonance frequency, $\nu_o = v_A/2\ell_{cor}$, the photospheric power spectrum, $< 1/2\ \rho v_\theta^2 >^{photo}_{\nu}$ could in itself actively depend upon $\underset{\sim}{B}_o$. In this regard, independent investigations of the role of magnetic fields in $\beta \gtrsim 1$ turbulence will be invaluable in shedding light upon the nature of the photospheric velocity field's spectral power as it appears in equations (60) and (61).

*(d) The Reactive Electrodynamic Response and the Role of Irreversibilities*

Since the majority of the magnetic loop system is found within the corona, this section will focus upon the reactive response of the *coronal* portion of magnetic loops to electrodynamic driving. Furthermore, I will assume that a local resonance absorption process is occurring within the corona since the local resonance condition is easily satisfied.

As I have already discussed, the power drain on the photospheric driver is explicitly independent of the dissipation -- a natural feature of resonance phenomena. This, however, does not mean that irreversibilities completely disappear from the problem. In fact, the root-mean square amplitude of the induced current, which is associated with the microscopic (i.e., electronic) and macroscopic (i.e., ionic) reactance of the plasma contained by the magnetic loop, does indeed depend upon irreversible processes such as electron-ion collisions. The microscopic reactance is related to the field-aligned current density, $j_{\parallel}$, which is carried by the electrons drifting at velocity $v_d$ along the ambient field. The macroscopic reactance is related to the cross-field current density, $j_{\perp}$, which through Lorentz forces drives an azimuthal flow of coronal plasma with velocity $v_\theta$. Noting that the dominant drag on the ions is viscous drag whereas for electrons it is Joule drag, it follows that the ratio of ion to electron heating is the ratio of the viscous resistance to the Joule resistance, i.e.,

$$\frac{\text{viscous ion heating}}{\text{Joule electron heating}} \simeq \frac{R_{\text{viscous}}}{R_{\text{Joule}}} \simeq Pr_{\text{mag}} \simeq \beta\left(\frac{m_i}{m_e}\right)^{1/2}\left(1+\frac{\nu_i^2}{\Omega_i^2}\right)^{-1} \qquad (62)$$

where $R_{\text{viscous}}$ represents viscous drag on the azimuthal flow of plasma and where $R_{\text{Joule}}$ represents "Joule" drag on the field-aligned flow of

electrons (c.f., section II. (b)). Again, there appears to be no explicit dependence upon irreversibilities such as collision frequencies. The appearance of irreversible phenomena is, however, explicit in expressions for the electron drift speed, $v_d$, the plasma's azimuthal flow velocity, $v_\theta$, and the width $(\Delta x_r)_{cor}$ of the coronal field lines which are subject to electrodynamic activity.

The width $(\Delta x_r)_{cor}$ can be easily estimated by noting that a magnetic loop responds at frequencies other than its global resonance frequency, $\omega_o$, given by equation (38). In fact the loop will respond for a continuum of different frequencies, $\Delta\omega_o \sim \omega_o/Q_{global}$, where $Q_{global}$ is the global quality of the entire loop system defined by equation (46). As one might expect, $\Delta\omega_o$ results in a continuum of excited spatial resonances whose overall thickness $(\Delta x_r)_{cor}$, is given by

$$(\Delta x_r)_{cor} = \frac{\Delta x_r}{R_{cor}\, Q_{global}} \tag{63}$$

where it is understood that $R_{cor}^{-1}$ represents the local quality of the coronal portion of the magnetic loop given by equation (45) and where in this case, $\Delta x_r$ represents the width of a single spatial resonance within the corona given by equation (26).

The electron drift speed, $v_d$, is estimated by noting that,

$$I^2 R_{global} \cong \pi \sqrt{C/L}\, \langle \mathcal{E}^2 \rangle_{\nu_o}\, \nu_o \tag{64}$$

with $I = I_{\perp} = I_{\parallel} = \pi \ell_{\perp} (\Delta x_r) j_{\parallel}$ from equation (34). Since $j_{\parallel} = nev_d$, it simply follows from equation (64) that the electron drift speed normalized to the ion sound speed is given by,

$$\left(\frac{v_d}{v_s}\right)_{cor} \simeq 1.1 \times 10^2 \left(\frac{B_{photo}}{B_o}\right) \left(\frac{T_{eff}}{T}\right) \left(\frac{\delta_{skin}}{a}\right) R_{cor}^{-1} Q_{global}^{1/2} \left(\frac{v_\theta}{v_s}\right)_{photo} \quad (65)$$

where equations (26) and (59) have been used. In equation (65) $v_s$ represents the ion sound speed, $B_{photo}/B_o$ and $T_{eff}/T$ represents the ratio of the photospheric magnetic field to the coronal field and the ratio of the photospheric temperature to the coronal loop temperature, $\delta_{skin}/a$ represents the ratio of the plasma skin depth (i.e., $\delta_{skin} \equiv c/\omega_{pe}$) to the Alfven speed's scale length (c.f., equation (25)), $R_{cor}$ is the normalized coronal resistance given by equation (45), $Q_{global}$ is the global quality of the magnetic loop system defined by equation (46) and $(v_\theta)_{photo}$ represents the velocity of the photospheric driver (i.e. $v_\theta \sim \sqrt{(v_\theta^2)_{\nu_o} \nu_o}$. If we assume that the coronal resistance dominates both the chromospheric and photospheric resistance -- a situation which occurs for solar applications (c.f., section III), then $Q_{global} \sim R_{cor}^{-1}$ and equation (65) can be written as

$$\left(\frac{v_d}{v_s}\right)_{cor} \simeq 62.1 \left(\frac{B_{photo}}{B_o}\right) \left(\frac{T_{eff}}{T}\right) \left(\frac{\delta_{skin}}{\ell_{\perp}}\right) \left(1 + Pr_{mag}\right)^{-1/2} Re_{mag}^{1/2} \left(\frac{v_\theta}{v_s}\right)_{photo} \quad (66)$$

where equation (45) for $R_{cor}$ has been used. For the case of solar magnetic loops, equation (66) can be further simplified by noting that $B_{photo}/B_o \simeq 3.38$, $T_{eff}/T \simeq 2 \times 10^{-3}$, $\delta_{skin}/\ell_{\perp} \simeq 10^{-8}$, and $a \simeq \ell_{\perp}$, i.e.,

$$\left(\frac{v_d}{v_s}\right)^{solar}_{cor} \simeq 4.2 \times 10^{-9} \left(1 + Pr_{mag}\right)^{-1/2} Re^{1/2}_{mag} \left(\frac{v_\theta}{v_s}\right)_{photo} . \qquad (67)$$

The azimuthal flow velocity, $(v_\theta)_{cor}$, is estimated by noting that,

$$1/2\ C\ \phi^2\ \omega_o \simeq Q_{global}\ I^2 R_{global} \qquad (68)$$

where $\phi \simeq (v_\theta)_{cor} B_o \ell_\perp / c$ is the coronal loop's capacitive emf. Equation (68) results in the following expression for the coronal flow velocity, normalized to the coronal ion sound speed:

$$\left(\frac{v_\theta}{v_s}\right)_{cor} \simeq 2 \left(\frac{B_{photo}}{B_o}\right) \left(\frac{T_{eff}}{T}\right)^{1/2} Q^{1/2}_{global} \left(\frac{v_\theta}{v_s}\right)_{photo} \qquad (69)$$

which, for the solar parameters used earlier, reduces to

$$\left(\frac{v_\theta}{v_s}\right)^{solar}_{cor} \simeq 0.25 \left(1 + Pr_{mag}\right)^{-1/6} Re^{1/6}_{mag} \left(\frac{v_\theta}{v_s}\right)_{photo} . \qquad (70)$$

The size of the solar coronal region within which the resistive and reactive activity described by equations (61), (66) and (70) occurs is given by equation (63) for $(\Delta x_r)_{cor}$

$$\frac{(\Delta x_r)_{cor}}{\ell_\perp} = \pi^{1/3} \left(1 + Pr_{mag}\right)^{1/3} Re^{-1/3}_{mag} \qquad (71)$$

where equation (26) for the width of a single resonance, $\Delta x_r$, has been used along with $Q_{global} \sim R^{-1}_{cor}$.

(c) Nonlinear Effects

Knowledge of the plasma reactance derived by a linear formalism is very useful in determining the relevance of various nonlinear processes. For example, microscopic nonlinearities associated with the destablization of the field-aligned electron current could result in an anomalous increase in the electron collision frequency, $\nu_{anomalous}$, given by equation (14). Such microscopic nonlinearities can only occur if $(v_d/v_s)_{cor} > 1$ and would result in both anomalous current dissipation and anomalous viscous dissipation. Since the magnetic Prandtl number, $Pr_{mag}$, as derived from viscous dissipation of sheared, incompressible flows, depends upon the ion collision frequency which in turn depends upon the electron collision frequency (c.f., equation (11)), it follows that the anomalous Prandtl number, $Pr_{mag}^{anomalous}$, is given by

$$Pr_{mag} \rightarrow Pr_{mag}^{anomalous} \simeq \beta \left(\frac{m_i}{m_e}\right)^{1/2} \left(1 + \left(\frac{m_e}{m_i}\right)\left(\frac{\omega_{pi}^2}{\Omega_i^2}\right)\right)^{-1} \qquad (72)$$

where $\nu_{anomalous} \simeq \omega_{pi}$ has been used (i.e., equation (14)). Thus the ratio of ion to electron heating described by equation (62) could be significantly affected by the onset of microscopic plasma turbulence. In addition, the thermal vs. nonthermal energy partitioning of the "heated" electrons is affected, with the nonthermal component becoming increasingly enhanced as the ratio $(v_d/v_s)_{cor}$ increases beyond unity (c.f., Ionson, 1981). The width of the spatial resonance, $\Delta x_r$, would also be increased since the magnetic Reynold's number, $Re_{mag}$, depends upon the electron collision frequency. In fact, $Re_{mag}$

would decrease with the development of microscopic plasma turbulence also resulting in a decrease in the macroscopic flow velocity, $(v_\theta)_{cor}$, described by equation (70).

A second possible nonlinearity that could develop would be driven by the macroscopic flow field, $(v_\theta)_{cor}$. Although for a linear analysis this is a sheared flow, a compressible component could be generated if $(v_\theta/v_s)_{cor} \sim 1$. In this case it would be necessary to consider viscous heating of compressible flows which is much more efficient than viscous heating of sheared flows (c.f., Hollweg, 1979). In fact the relevant coefficient of viscosity used in deriving the magnetic Prandtl number would be $\mu_{||}$ rather than $\mu_\perp$. Therefore, if $(v_\theta/v_s)_{cor} \sim 1$ then the magnetic Prandtl number, $Pr_{mag}^{compressible} \simeq \beta(m_i/m_e)^{1/2}\,(\Omega_i^2/\nu_i^2)$. In general however, the flow is not completely compressible. Since $(v_\theta/v_s)_{cor}^2$ is a measure of compressibility, the effects of compressibility can be approximated by using the following expression for the Prandtl number:

$$Pr_{mag} \rightarrow Pr_{mag}^{compressible} \simeq \beta \left(\frac{m_i}{m_e}\right)^{1/2} \left(\frac{\Omega_i}{\nu_i}\right)^2 \left(\frac{v_\theta}{v_s}\right)_{cor}^2 . \qquad (73)$$

This could also significantly affect the ratio of ion to electron heating as well as the width of the spatial resonance, $\Delta x_r$.

It is quite clear that the ion to electron heating rate depends critically upon the plasma conditions of the system of interest as well as whether or not microscopic and/or macroscopic nonlinearities develop. Note that if both types

of nonlinearities occur, then the anomalous ion collision frequency, $\nu_i \rightarrow (m_e/m_i)^{1/2}\,\omega_{pi}$, should be used in equation (73). It is important to note that the question of nonlinearities can only be properly addressed by first investigating the linear response -- specifically, the reactance discussed in section II. d. It will become apparent in the next section that applications to solar coronal loops will require nonlinear modifications.

## III. Solar Applications

In order to apply the physics of electrodynamic coupling described in section II., it is necessary that we have some knowledge of the magnetothermodynamic conditions characteristic of the particular plasma setting of interest. As a *demonstration* of how this physics can be utilized, a specific application to solar magnetic loop systems will be presented.

### (a) *Resonant Electrodynamic Heating of Solar Coronal Loops*

Serio et al. (1980) have recently generalized the scaling laws derived by Rosner et al. (1978) to include solar coronal loops whose height exceeds their pressure scale height. These scaling laws, which are fairly consistent with observations are given by

$$T \simeq 1.4 \times 10^3 \,(P\ell_{cor})^{1/3} \exp\left(\frac{-0.04\ell_{cor}}{\ell_p}\right)\ {}^{o}K \qquad (74)$$

$$E_{loss} \simeq 10^5\, P^{1.17}\, \ell_{cor}^{-0.83} \exp\left(\frac{-0.5\ell_{cor}}{\ell_p}\right)\left(\frac{ergs}{cm^3\text{-}sec}\right) \qquad (75)$$

where T is the maximum temperature of the coronal loop, P the base pressure, $\ell_p \simeq 6.12 \times 10^3 T$ cm, the pressure scale height and where $E_{loss}$ is the average

energy per unit volume that is lost through chromospheric and coronal radiation. In equations (74) and (75) it has been assumed that the energy deposition scale height is large compared to the loop length since we are dealing with a global heating mechanism.

Golub et al. (1980) have also derived an empirical relationship between the base pressure of coronal loops and the average strength of the underlying photospheric magnetic field, $B_{photo}$. Assuming that the coronal magnetic field, $B_o$, can be estimated by a simple dipole extrapolation of $B_{photo}$ (i.e., $B_o/B_{photo} \simeq (2\ell_{cor}/2\ell_{cor} + \ell_{cor})^3 \simeq 0.296$ with a dipole displacement of $2\ell_{cor}$), their relationship becomes,

$$P = 2.1 \times 10^{-2} B_o^{1.6} \left(\frac{\text{dynes}}{\text{cm}^2}\right) \tag{76}$$

From equations (74) and (76) it is possible to determine the magnetothermodynamic state of a coronal loop as a function of its maximum temperature, T, and length, $\ell_{cor}$. Specifically,

$$P = 3.64 \times 10^{-10} \left(\frac{T^3}{\ell_{cor}}\right) \exp\left(\frac{1.2\ell_{cor}}{\ell_p}\right) \left(\frac{\text{dynes}}{\text{cm}^2}\right) \tag{77}$$

$$B_o = 1.41 \times 10^{-5} \left(\frac{T^{1.875}}{\ell_{cor}^{0.625}}\right) \exp\left(\frac{0.75\ell_{cor}}{\ell_p}\right) \text{ (gauss)} \tag{78}$$

and, noting an exponential drop in the coronal density with height, the coronal Alfven speed is given by,

$$v_A = 2.68 \times 10^3 \left(\frac{T^{0.875}}{\ell_{cor}^{0.125}}\right) \exp\left(-\frac{0.174\ell_{cor}}{\ell_p}\right)\left(\frac{cm}{sec}\right) \qquad (79)$$

In order that the temperature, T, can be eliminated from equations (77) - (79) it is necessary to utilize equation (75) for $E_{loss}$, noting that

$$E_H = E_{loss} \qquad (80)$$

where $E_H$ is the generalized electrodynamic heating function given by equation (55). A simultaneous solution of equations (77) - (80) will then result in a scaling of loop temperature, T, and base pressure, P, with the loop size, $\ell_{cor}, \ell_\perp$, and the spectral power of the photospheric velocity field, $< 1/2\ \rho v_\theta^2 >_\nu^{photo}$ (i.e., goal (ii) as stated in the Introduction).

To determine the relevant form of electrodynamic heating (i.e., resonant or nonresonant) it is first necessary to estimate the global quality, $Q_{global}$, of the loops. This can be easily done by using the following parameters as estimates in equations (27), (44) - (46).

$$\tau_{photo} = \frac{4\pi\,\nu_{e\text{-}n}}{\omega_{pe}^2} \sim 5.9 \times 10^{-12}\ \text{sec};\ v_A^{photo} \sim 10^6\ \text{cm/sec};\ \ell_{photo} \sim 5 \times 10^7\ \text{cm};\ \beta_{photo}$$

$$\tau_{chrom} = \frac{4\pi\,\nu_{e\text{-}i}}{\omega_{pe}^2} \sim 2 \times 10^{-13}\ \text{sec};\ v_A^{chrom} \sim 3 \times 10^6\ \text{cm/sec};\ \ell_{chrom} \sim 5 \times 10^7\ \text{cm};\ \beta_{chrom}$$

$$\tau_{cor} = \frac{4\pi\,\nu_{e\text{-}i}}{\omega_{pe}^2} \sim 5 \times 10^{-17}\ \text{sec};\ v_A \sim 6 \times 10^7\ \text{cm/sec};\ \ell_{cor} \sim 10^{10}\ \text{cm};\ \beta_{cor} \sim 0.1$$

$$a \sim \ell_\perp \sim 0.1\ \ell_{cor}$$

The results are:

$$Re_{mag}^{photo} \sim 4 \times 10^{7}; \; R_{photo} \sim 10^{-9}$$

$$Re_{mag}^{chrom} \sim 4 \times 10^{9}; \quad Pr_{mag}^{chrom} \sim 43; \; R_{chrom} \sim 2 \times 10^{-9}$$

$$Re_{mag}^{cor} \sim 2 \times 10^{12}; \; Pr_{mag}^{cor} \sim 4.3; \; R_{cor} \sim 2 \times 10^{-4}$$

$$\sqrt{L/C} \sim 0.24 \text{ Ohms}$$

$$Q_{global} \sim R_{cor}^{-1} \sim 5 \times 10^{3}$$

where it has bee.. assumed that local resonance absorption occurs within the corona (i.e., equation (45) for was used to estimate $R_{cor}$). The rationale for assuming that local resonance absorption occurs within the corona is based upon the fact that the global resonance frequency of the entire magnetic loop system depends primarily upon coronal rather than chromospheric and photospheric conditions (c.f., equation 38)).

It is quite obvious that the global quality of typical solar magnetic loops is extremely large (i.e., $Q_{global} \sim 3 \times 10^{3}$) -- at least under the constraints of a linear theory. Therefore, the resonant form of the heating

function, $E_H$, described by equation (61) should be used in the energy balance described by equations (75) and (80). This results in the following implicit equations for the maximum temperature, T, and base pressure, P:

$$T = 3.36 \times 10^4 \left[ T_{eff} \exp\left(0.36 \ell_{cor}/\ell_p\right) < 1/2 \rho v_\theta^2 >_{\nu_o}^{photo} \right]^{2/7} {}^{o}K \qquad (81)$$

$$P = \frac{1.38 \times 10^4}{\ell_{cor}} \exp\left(1.51\, \ell_{cor}/\ell_p\right) \left[ T_{eff} < 1/2\, \rho v_\theta^2 >_{\nu_o}^{photo} \right]^{6/7} \left(\text{dynes/cm}^2\right) \qquad (82)$$

where $R_{loop} \sim R_{global}$ has been used.

In order to solve equations (81) and (82) explicitly for T and P as a function of loop length, $\ell_{cor}$, it is necessary that we know the spectral power of the photospheric velocity field. As a demonstration, the power spectrum illustrated in Figure 3e has been assumed. This spectrum corresponds to observations of solar plage regions where densities are of the order of $10^{-7}$ gm/cm$^3$. Illustrated are two major peaks, one at intermediate periods ($300 > \tau > 100$ sec) (Orrall, 1966; Woods and Cram, 1981) and one at longer periods ($\tau > 400$ sec) (Harvey, 1980). Figure 3d illustrates how the global resonance period versus loop length scaling, $\tau_o = \tau_o(\ell_{cor})$, maps the spectral power function of the photospheric velocity field into $E_H = E_H(\ell_{cor})$ via equation (61) (c.f., Figure 3c), $T = T(\ell_{cor})$ via equation (81) (c.f., Figure 3b) and $P = P(\ell_{cor})$ via equation (82). Also plotted in Figures 3a and 3b are observations of active region loops (Landini et al., 1975; Pye et al., 1977) which absorb power from the "intermediate regime" of the photospheric spectral

FIG 3

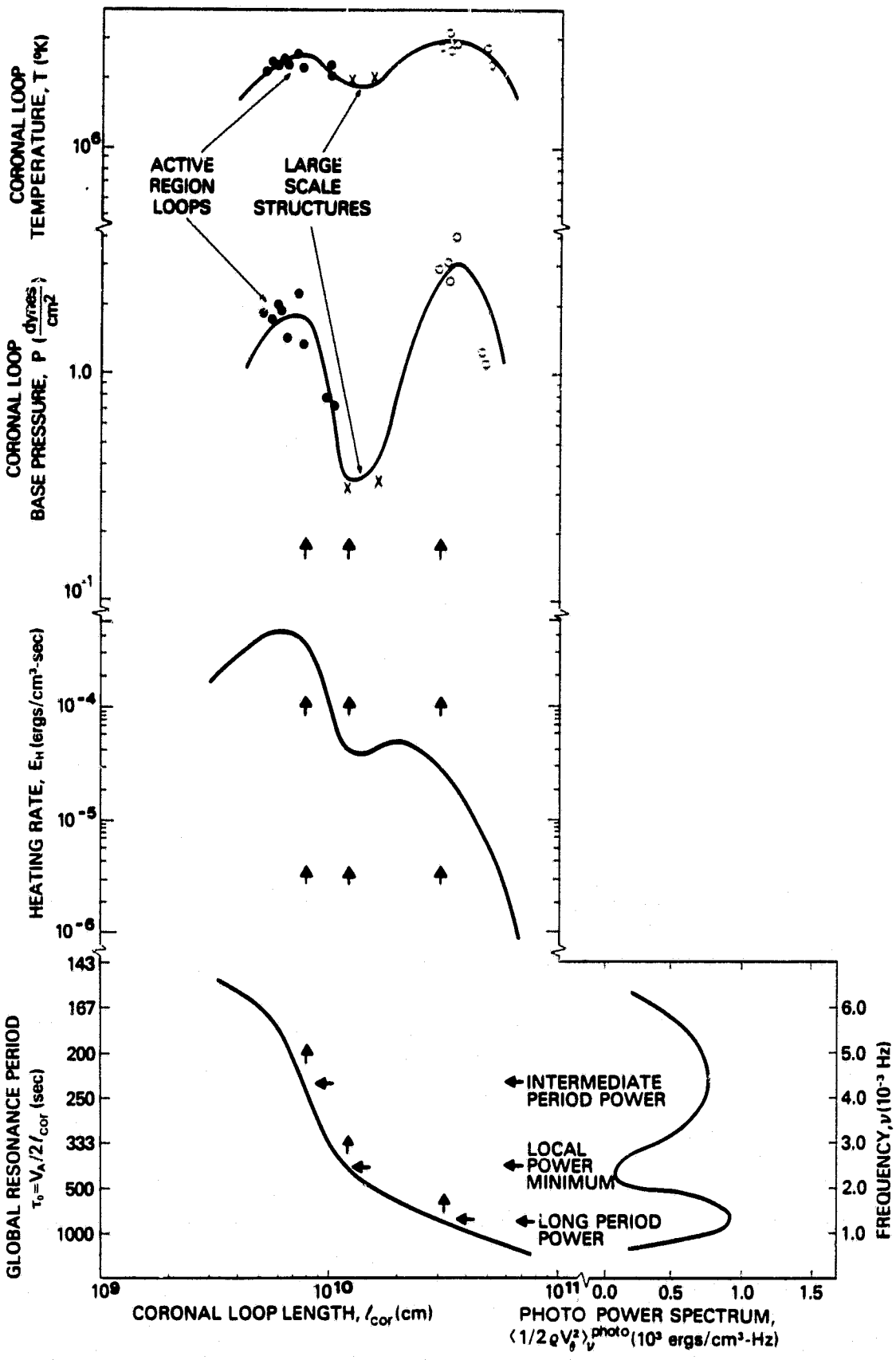
CORONAL LOOP TEMPERATURE, T (°K)
ACTIVE REGION LOOPS
LARGE SCALE STRUCTURES
CORONAL LOOP BASE PRESSURE, P (dynes/cm²)
HEATING RATE, $E_H$ (ergs/cm³-sec)
GLOBAL RESONANCE PERIOD $\tau_0 = V_A/2l_{cor}$ (sec)
143
167
200
250
333
500
1000
INTERMEDIATE PERIOD POWER
LOCAL POWER MINIMUM
LONG PERIOD POWER
FREQUENCY, ν(10⁻³ Hz)
CORONAL LOOP LENGTH, $l_{cor}$(cm)
PHOTO POWER SPECTRUM, $\langle 1/2\rho V_\theta^2 \rangle_\nu^{photo}$(10³ ergs/cm³-Hz)

power function; large-scale loop structures (Maxson and Vaiana, 1977) which are electrodynamically coupled to the "local power minimum" region of the photospheric spectral power function; and very large scale active loops (Pye et al., 1977) which can absorb power from the "long period" regime of the photospheric spectral power function.

(b) *The Reactive Response and the Role of Irreversibilities in Solar Coronal Loops*

Using the results of Fig. 3, Fig. 4 illustrates how the natural impedence, $\sqrt{L/C}$, magnetic Prandtl number, $Pr_{mag}$, and magnetic Reynold's number, $Re_{mag}$ of solar magnetic loops scales with the loop length, $\ell_{cor}$. Noting that $(v_\theta/v_s)_{photo} \sim 5 \times 10^{-2}$, these parameters are used in equations (45), (46), (67), (70) and (71) for $Q_{global}$, $(v_d/v_s)_{cor}$, $(v_\theta/v_s)_{cor}$ and $(\Delta x_r)_{cor}$ which were derived from a linear analysis, i.

$$Q_{global}^{linear} = \pi^{-1/3} (1 + Pr_{mag})^{-1/3} Re_{mag}^{1/3} \tag{83}$$

$$\left(\frac{v_d}{v_s}\right)_{cor}^{linear} \simeq 2.1 \times 10^{-10} (1 + Pr_{mag})^{-1/2} Re_{mag}^{1/2} \tag{84}$$

$$\left(\frac{v_\theta}{v_s}\right)_{cor}^{linear} \simeq 1.25 \times 10^{-2} (1 + Pr_{mag})^{-1/6} Re_{mag}^{1/6} \tag{85}$$

$$(\Delta x_r)_{cor}^{linear} \simeq 0.1 \ell_{cor}/Q_{global}^{linear} \tag{86}$$

FIG 4

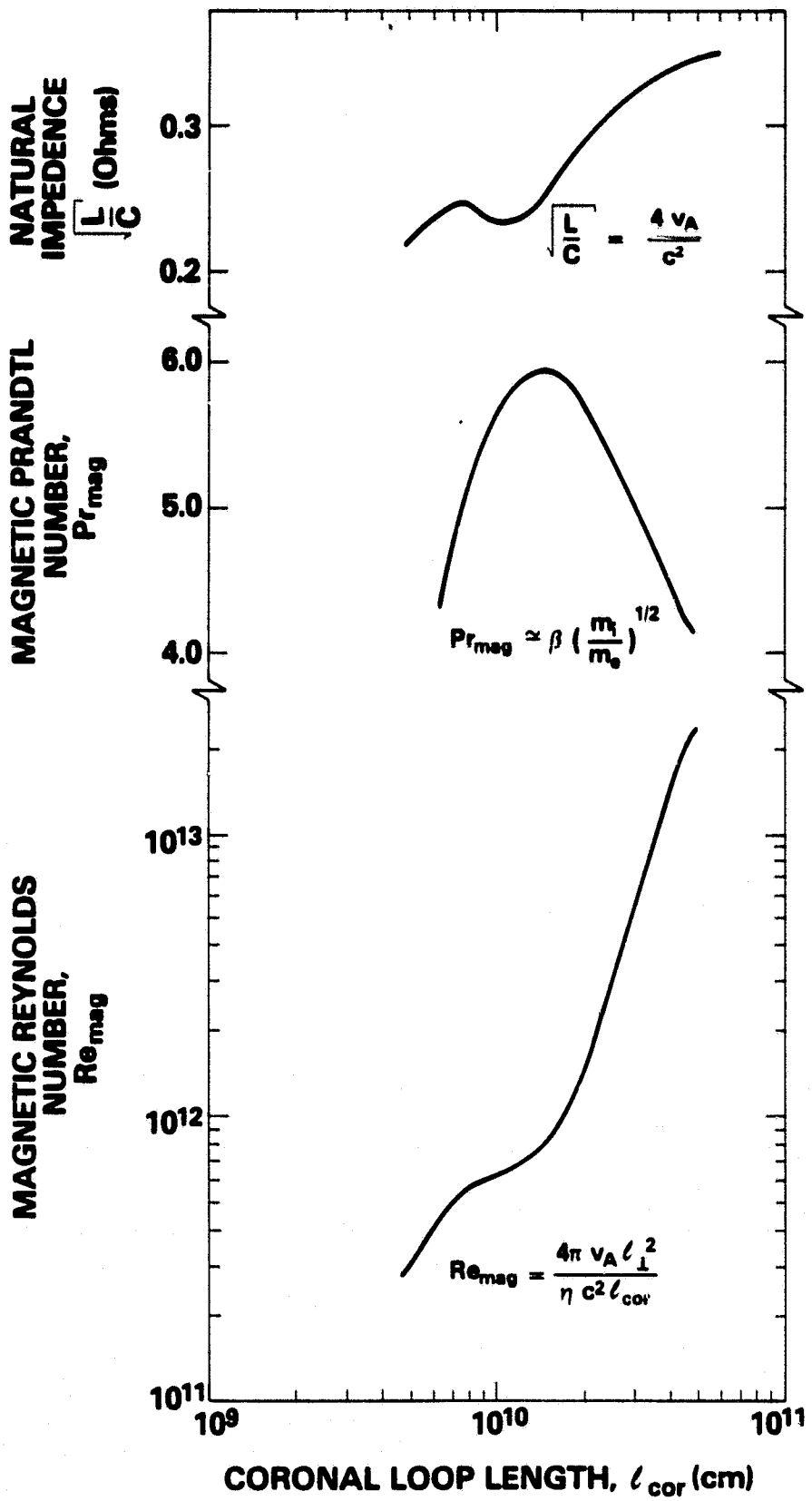
NATURAL IMPEDENCE $\sqrt{\frac{L}{C}}$ (Ohms)
0.3
0.2
$\sqrt{\frac{L}{C}} = \frac{4 v_A}{c^2}$
MAGNETIC PRANDTL NUMBER, $Pr_{mag}$
6.0
5.0
4.0
$Pr_{mag} \propto \beta \left(\frac{m_i}{m_e}\right)^{1/2}$
MAGNETIC REYNOLDS NUMBER, $Re_{mag}$
$10^{13}$
$10^{12}$
$10^{11}$
$Re_{mag} = \frac{4\pi v_A \ell_\perp^2}{\eta c^2 \ell_{cor}}$
$10^9$
$10^{10}$
$10^{11}$
CORONAL LOOP LENGTH, $\ell_{cor}$ (cm)

which yield the results illustrated in Figure 5. One noteworthy feature of this illustration is the extremely large Q-values leading one to believe that the microscopic and/or macroscopic reactance stemming from a linear theory could be quite appreciable. It is important to note from this figure that although microscopic nonlinearities associated with anomalous current dissipation are *unimportant* (i.e., because $(v_d/v_s)_{cor} \ll 1$) macroscopic nonlinearities associated with the conversion of a sheared, incompressible coronal flow into a partially compressible flow probably are important because $(v_\theta/v_s)_{cor} \sim 1$. This is consistent with Hollweg's (1981) independent analysis of the problem. Therefore, as discussed in section II.e., equation (73) for $Pr_{mag}^{compressible}$ should be used. This will result in increased viscous dissipation which lowers the Q-value of the loops, thereby resulting in both a broadened spatial resonance and a decrease in the coronal flow velocity, *i.e.*,

$$Q_{global}^{nonlinear} \simeq 1.6 \times 10^{-2} \; Pr_{mag}^{-1/12} \; Re_{mag}^{1/4} \tag{87}$$

$$\left(\frac{v_\theta}{v_s}\right)_{cor}^{nonlinear} \simeq 2.2 \times 10^{-3} \; Pr_{mag}^{-1/8} \; Re_{mag}^{1/8} \tag{88}$$

$$(\Delta x_r)_{cor}^{nonlinear} \simeq 0.1 \; \ell_{cor}/Q_{global}^{nonlinear} \tag{89}$$

Figure 6 illustrates the nonlinear reactance and Q-values described by equations (87) - (89) for the case of solar magnetic loops. Note that although the quality, $Q_{global}^{nonlinear}$, is significantly smaller than that estimated from a purely linear analysis, it is still larger than unity validating use of the resonant

FIG 5

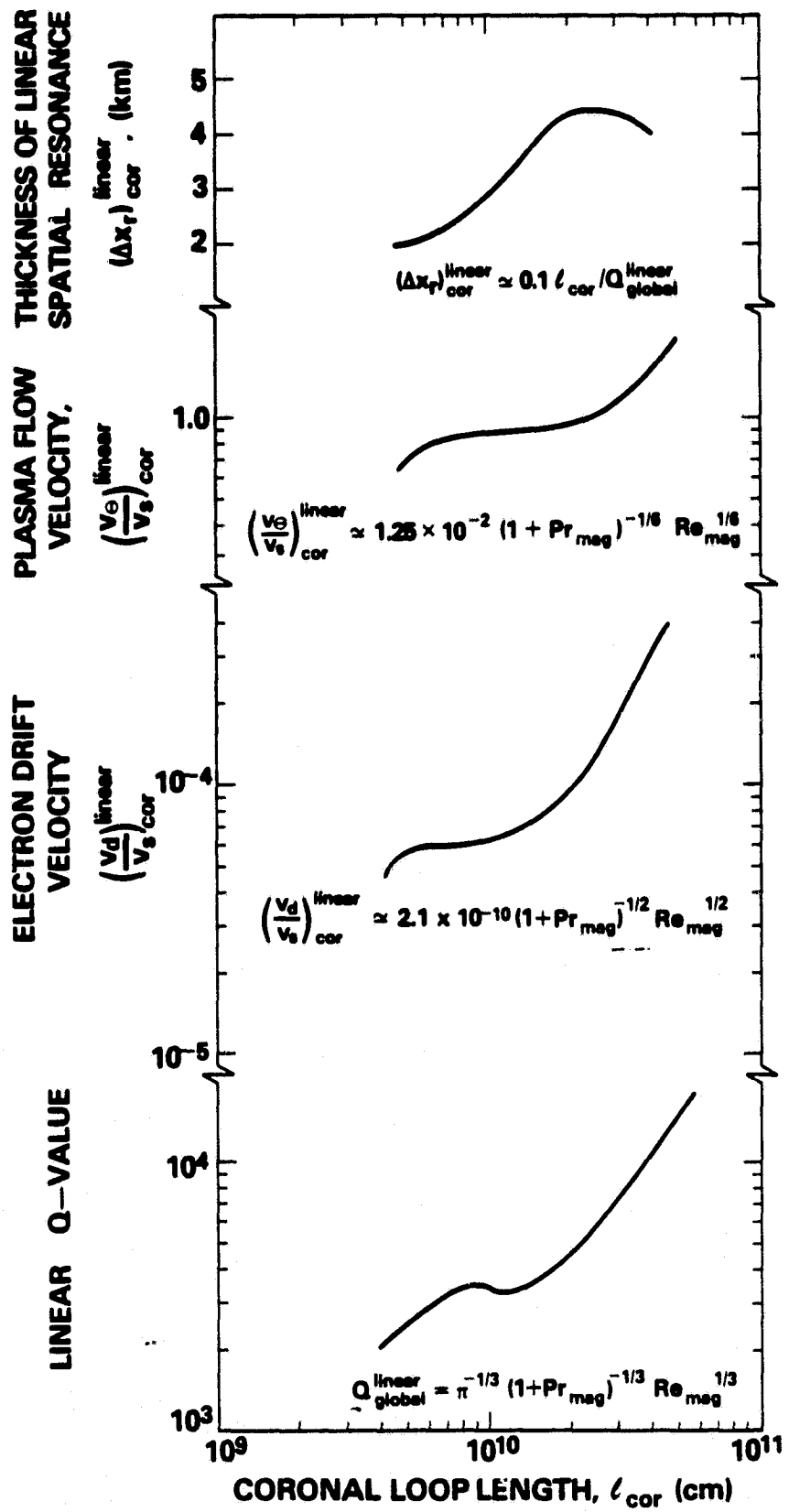
THICKNESS OF LINEAR SPATIAL RESONANCE
$(\Delta x_r)^{linear}_{cor}$, (km)
5
4
3
2
$(\Delta x_r)^{linear}_{cor} \simeq 0.1\,\ell_{cor}/Q^{linear}_{global}$
PLASMA FLOW VELOCITY, $\left(\frac{v_\Theta}{v_s}\right)^{linear}_{cor}$
1.0
$\left(\frac{v_\Theta}{v_s}\right)^{linear}_{cor} \simeq 1.25\times10^{-2}\,(1+Pr_{mag})^{-1/6}\,Re_{mag}^{1/6}$
ELECTRON DRIFT VELOCITY $\left(\frac{v_d}{v_s}\right)^{linear}_{cor}$
$10^{-4}$
$\left(\frac{v_d}{v_s}\right)^{linear}_{cor} \simeq 2.1\times10^{-10}(1+Pr_{mag})^{-1/2}\,Re_{mag}^{1/2}$
$10^{-5}$
LINEAR Q–VALUE
$10^4$
$Q^{linear}_{global} = \pi^{-1/3}\,(1+Pr_{mag})^{-1/3}\,Re_{mag}^{1/3}$
$10^3$
$10^9$
$10^{10}$
$10^{11}$
CORONAL LOOP LENGTH, $\ell_{cor}$ (cm)

heating function, $E_H$. This must be so since it is the resonant characteristics of the system which nonlinearly supports the compressibility of the flow. Therefore, the results depicted in Figures 3 and 4 remain unchanged.

As is evident in Figure 6a, the cross-field size of the coronal dissipation site has dramatically increased from the order of kilometers (c.f., Figure 5a and Ionson, 1977, 1978) to the order of *thousands* of kilometers due to the nonlinear modifications presented here. This is an extremely important result since there has been a great deal of concern regarding how solar coronal loops can be heated throughout their entire volume (c.f., Hollweg, 1979).

Another interesting feature of this analysis is the prediction of an 11-16 km/sec coronal velocity field (c.f., Figure 6b) and the preferential viscous heating of the ions, i.e.,

$$\frac{\text{viscous ion heating}}{\text{Joule electron heating}} \simeq Pr_{mag}^{compressible} \sim 10^8 \qquad (90)$$

Both of these effects could be responsible for the widespread observations of coronal line broadening (c.f., Feldman and Behring, 1974; Acton et al., 1981).

## IV. Conclusion

The major emphasis of this article has been the physics of global electrodynamic coupling between a $\beta<1$ magnetic loop and an underlying $\beta>1$ mechanical energy reservoir. A rigorous analysis of this problem has revealed that the physics can be represented by a simple yet equivalent LRC circuit analogue. This analogue points to the existence of global structure oscillations (i.e., $\nu_o = v_A/2\ell_{cor}$) which resonantly

FIG 6

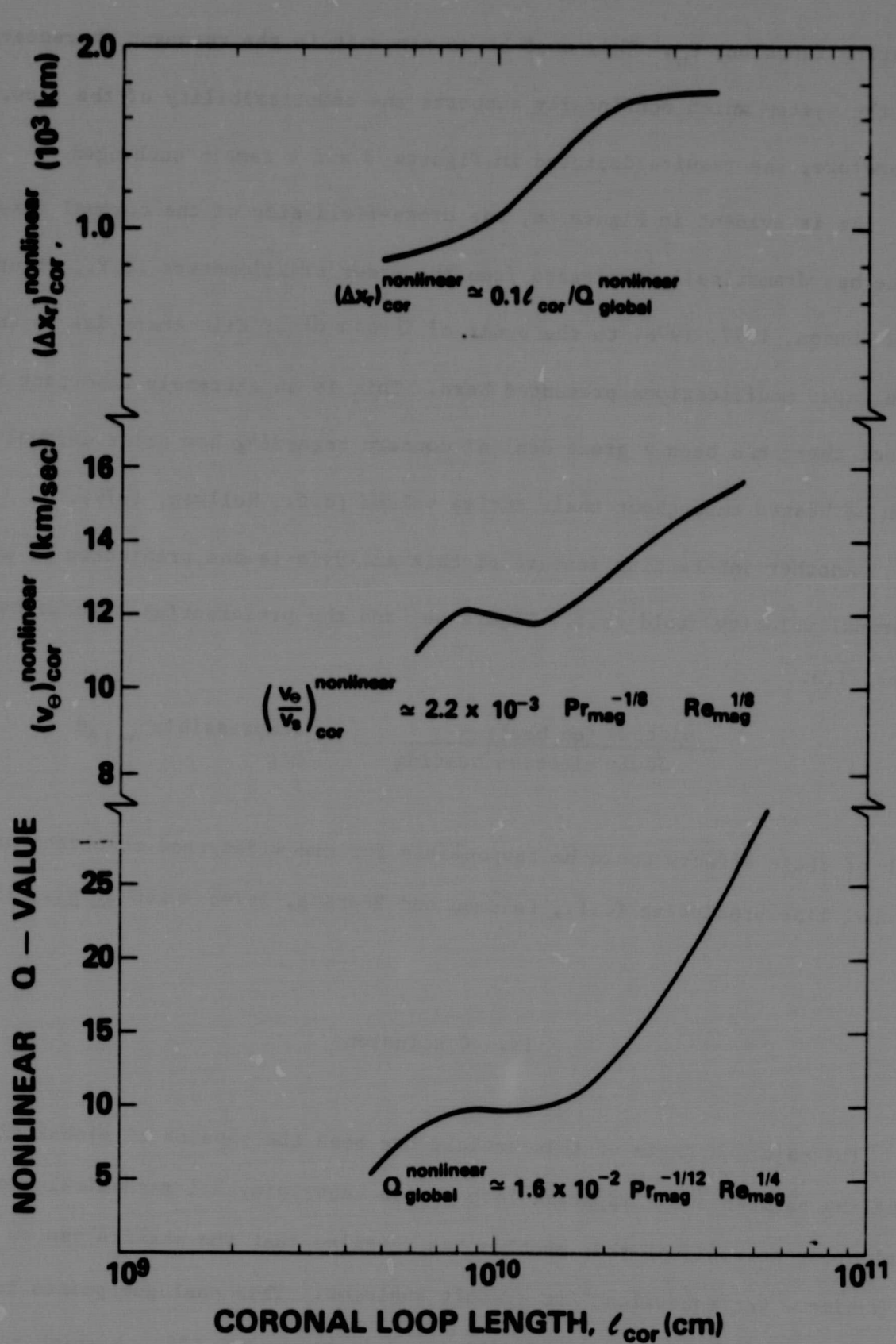
PLASMA FLOW VELOCITY, $(v_e)_{cor}^{nonlinear}$ (km/sec)
THICKNESS OF NONLINEAR SPATIAL RESONANCE $(\Delta x_r)_{cor}^{nonlinear}$ ($10^3$ km)
NONLINEAR Q – VALUE
2.0
1.0
16
14
12
10
8
25
20
15
10
5
$(\Delta x_r)_{cor}^{nonlinear} \simeq 0.1 \ell_{cor} / Q_{global}^{nonlinear}$
$\left(\frac{v_e}{v_s}\right)_{cor}^{nonlinear} \simeq 2.2 \times 10^{-3} \; Pr_{mag}^{-1/8} \; Re_{mag}^{1/8}$
$Q_{global}^{nonlinear} \simeq 1.6 \times 10^{-2} \; Pr_{mag}^{-1/12} \; Re_{mag}^{1/4}$
$10^9$
$10^{10}$
$10^{11}$
CORONAL LOOP LENGTH, $\ell_{cor}$ (cm)

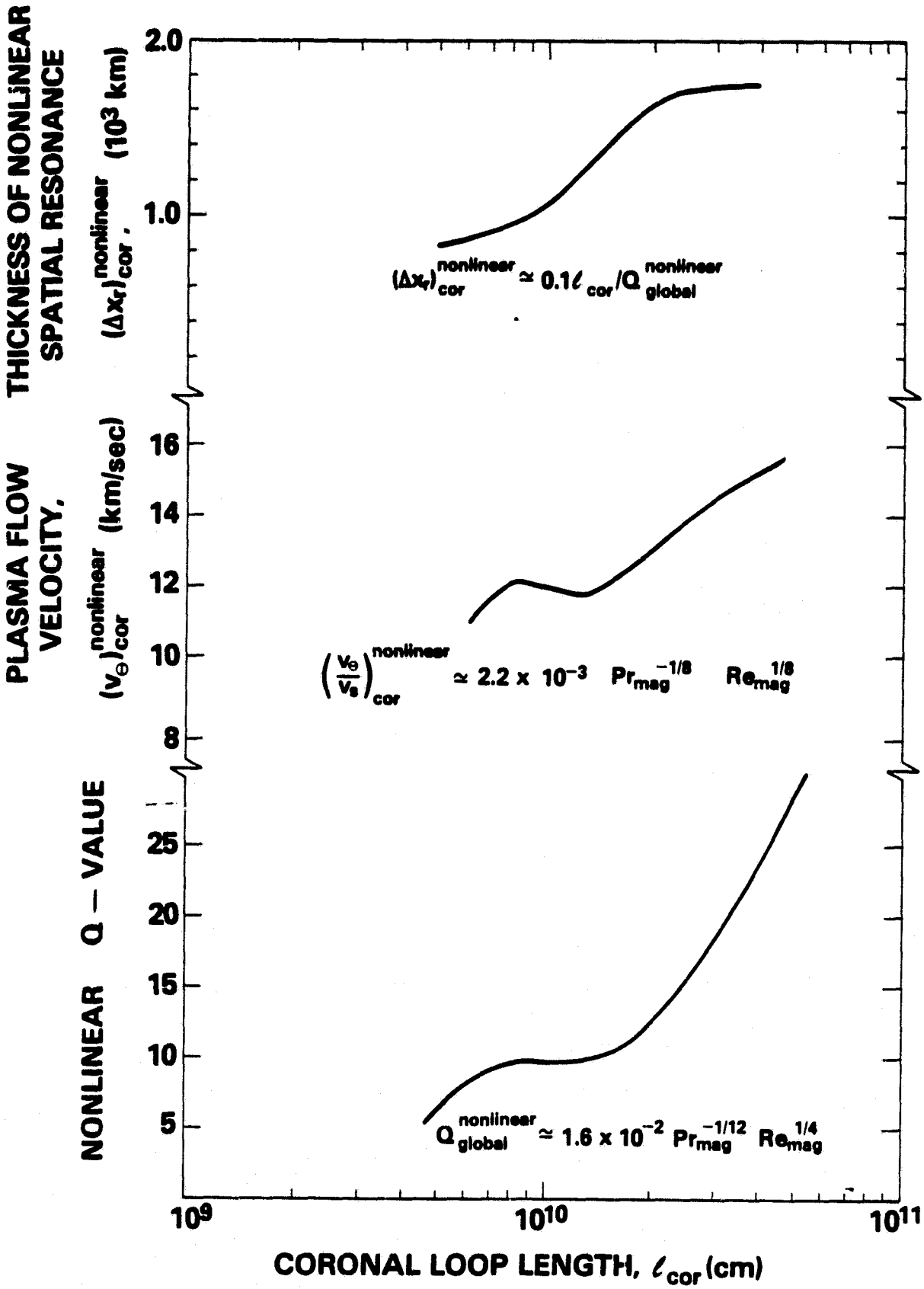
THICKNESS OF NONLINEAR SPATIAL RESONANCE
$(\Delta x_r)^{nonlinear}_{cor}$, $(10^3$ km)
2.0
1.0
$(\Delta x_r)^{nonlinear}_{cor} \simeq 0.1 \ell_{cor} / Q^{nonlinear}_{global}$
PLASMA FLOW VELOCITY,
$(v_\Theta)^{nonlinear}_{cor}$ (km/sec)
16
14
12
10
8
$\left(\frac{v_\Theta}{v_s}\right)^{nonlinear}_{cor} \simeq 2.2 \times 10^{-3} \; Pr_{mag}^{-1/8} \; Re_{mag}^{1/8}$
NONLINEAR Q – VALUE
25
20
15
10
5
$Q^{nonlinear}_{global} \simeq 1.6 \times 10^{-2} \; Pr_{mag}^{-1/12} \; Re_{mag}^{1/4}$
$10^9$
$10^{10}$
$10^{11}$
CORONAL LOOP LENGTH, $\ell_{cor}$ (cm)

excite internal field line oscillations at a spatial resonance within the magnetic loop (i.e., $\Delta x_r$ being the width of the spatial resonance). Although the width of this spatial resonance as well as the induced currents, $j_{||}$ and $j_r$ explicitly depend upon viscosity and resistivity, the *resonant* form of the generalized electrodynamic heating function, $E_H$, is virtually independent of irreversibilities. This is a classic feature of high quality resonators that are externally driven by a broad band source of spectral power. This follows from the fact that at resonance the heating function depends solely upon the resistance, R, and the emf which can *interact* with the loop, $<\mathcal{E}^2>_{\nu_o}\Delta\nu_o$, i.e., $E_H \propto <\mathcal{E}^2>_{\nu_o}\Delta\nu_o/R$. Since the interaction bandwidth, $\Delta\nu_o$, also depends upon the resistance, i.e., $\Delta\nu_o/\nu_o \sim 1/Q = R\sqrt{C/L}$, it follows that $E_H \propto <\mathcal{E}^2>_{\nu_o}\nu_o/\sqrt{L/C}$ which is explicitly independent of R. In addition, since $<\mathcal{E}^2>_{\nu_o} \propto <\frac{1}{2}\rho v^2>_{\nu_o}$ it becomes clear how the heating function scales with the spectral power function of the mechanical driver. The essential feature of a resonant heating mechanism is that magnetic loops with different lengths and hence different global resonance frequencies are heated at a rate that critically depends upon the amount of $\beta \gtrsim 1$ spectral power at the resonance frequency, $\nu_o$.

As a demonstration, this physics was applied to the solar setting. A linear analysis resulted in extremely large Q-values for solar coronal loops implying very narrow spatial resonances of the order of kilometers and a coronal flow velocity of the order of the sound speed. The electron drift velocity was found to be orders of magnitude less than the ion sound speed and therefore microscopic plasma instabilities were not important. However, in light of the large coronal flow velocity it was necessary to consider nonlinear modifications to the linear analysis stemming from the development of a compressible component to the coronal flow. The nonlinearly generated compressible component of the flow allows the use of a viscosity coefficient which dramatically increases the rate of viscous dissipation. As such, the steady

state quality of solar coronal loops is decreased to Q~15 which results in broad spatial resonances of the order of thousands of kilometers, a coronal velocity field of the order of 10-16 km/sec and preferential viscous heating of the ions. The nonlinear modifications, however, do not change the temperature (pressure) scaling of solar coronal loops with their length. This follows from the fact that the system is still highly resonant (i.e., Q>1) allowing one to utilize the resonant form of the heating function derived from a linear analysis. It is remarkable that such a simple theory is so consistent with a variety of observational constraints, despite the neglect of nonlinearities other than those addressed in this article.

Acknowledgments

I would like to acknowledge extremely valuable conversations with Drs. J. Hollweg, L. Golub, R. Rosner, D. Spicer and G.S., Vaiana. I especially thank Dr. P.J.Morrison for his help in clarifying many of the subtle points which occurred throughout the course of this work.

## REFERENCE

Acton, L. W., Culhane, J. L., Gabriel, A. H., Wolfson, C. J., Rapley, C. G., Phillips, K. J. H., Antonucci, E., Bentley, R. D., Hayes, R. W., Joki, E. G., Jordan, C., Kayat, M. A., Kent, B., Leibacher, J. W., Nobles, R. A., Parmar, A. N., Strong, K. T. and Veck, N. J., 1981, Ap. J. (Letters), in press.

Alfven, A. 1977, Rev. of Geoph. and Space Physics, 15, 271.

Feldman, U., and Behring, W. E., 1974, Ap. J., Ap. J. (Letters), 189, L45.

Golub, L., Maxson, C., Rosner, K., Serio, S. and Vaiana, G. S. 1980, Ap. J., 238, 343.

Harvey, J. 1980, (Private communication).

Hasegawa, A. and Chen, L. 1976, Phys. Fluids, 19, 1924.

Hinata, S. 1980, Ap. J., 235, 258.

Hollweg, J. 1979, Proc. Skylab Workshop on Active Regions, Ch. 8, ed. F. Orrall.

Hollweg, J., 1981, Private communication.

Hollweg, J. 1981, Solar Physics, in press.

Ionson, J. A. 1977, Thesis Univ. Maryland.

Ionson, J. A. 1978, Ap. J., 226, 650.

Ionson, J. A., Ong, R.S.B., and Fontheim, F. G., 1979, Planet, Space Sci., 27, 203.

Ionson, J. A., 1981, in preparation.

Kappraff, J. M., and Tataronis, J. A., 1977, J. Plasma Physics, 18, 209.

Kuperus, M., Ionson, J. A., and Spicer, D. S., 1981, Ann. Rev. Astron. Astrophysics, 19.

Landini, M., Fossi, B. C. M., Krieger, A., and Vaiana, G. S., 1975, Solar Physics, 44, 69.

Malville, J. M., and Schindler, M., 1981, Solar Physics, in press.

Maxson, C. W., and Vaiana, G. S., 1977, Ap. J., 215, 919

Orrall, F. Q., 1966, Ap. J., 143, 917.

Ott, E., Wersinger, J., and Bonoli, P., 1978, Phys. Fluids, 21, 2306.

Papadopoulos, K., 1977, Rev. Geophys. Space Phys., 15, 113.

Pye, J. P., Evans, K. D., Hutcheon, R. J., Gerassimenko, M., Davis, M., Krieger, A. S., and Vesecky, J. F., 1978, Ap. J., 65, 123.

Rosner, R., Golub, L., Coppi, B. and Vaiana, G. S., 1978, Ap. J., 222, 317.

Rosner, R., Tucker, W. H., and Vaiana, G. S., 1978, Ap. J., 220, 643.

Serio, S., Peres, G., Vaiana, G. S., Golub, L., and Rosner, R., 1981, Ap. J., in press.

Vaiana, G. S., and Rosner, R., 1978, Ann. Rev. Astron. Astrophys., 16, 393.

Wentzel, D. G., 1978, Rev. Geophys. Space Science, 16, 757.

Wentzel, D. G., 1979, Ap. J., 227, 319.

Withbroe, G. L., and Noyes, R. W., 1977, Ann. Rev. Astron. Astrophysics, 15, 363.

Woods, D. T. and Cram, L. E., 1981, Solar Physics, in press.

## Figure Captions

Figure 1. Prototype magnetic loop system and equivalent LRC circuit.

Figure 2. Power factor, $p_f(\omega)$, versus the frequency normalized to the resoance frequency, $\omega_o$.

Figure 3. Illustration of how the solar photospheric power spectrum electrodynamically couples to coronal loops. The data points refer to active region loops (i.e., X's ; Landini et al., 1975; Pye et al., 1977), large-scale structures (i.e., crosses; Maxson and Vaiana, 1977) and very large scale active loops (i.e., circles; Pye et al., 1977).

Figure 4. Characteristic properties of solar coronal loops with $\ell_\perp/\ell_{cor} \simeq 0.1$.

Figure 5. Results of a linear analysis applied to solar coronal loops.

Figure 6. Results of a nonlinear analysis applied to solar coronal loops.

James A. Ionson: Laboratory for Astronomy and Solar Physics, NASA Goddard Space Flight Center, Greenbelt, MD 20771.